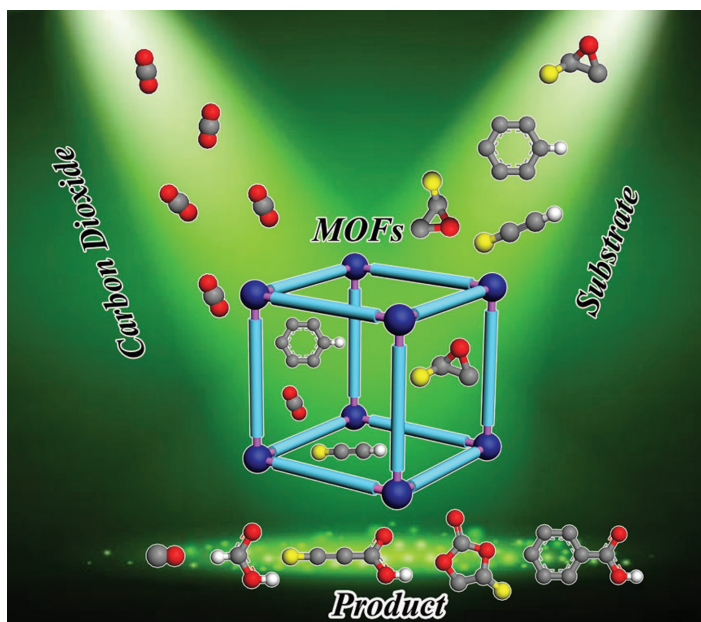# Metal-Organic Frameworks for CO$_2$ Chemical Transformations

Hongming He, Jason A. Perman, Guangshan Zhu,* and Shengqian Ma*

From the Contents

*C*arbon dioxide (CO$_2$), as the primary greenhouse gas in the atmosphere, triggers a series of environmental and energy related problems in the world. Therefore, there is an urgent need to develop multiple methods to capture and convert CO$_2$ into useful chemical products, which can significantly improve the environment and promote sustainable development. Over the past several decades, metal-organic frameworks (MOFs) have shown outstanding heterogeneous catalytic activity due in part to their high internal surface area and chemical functionalities. These properties and the ability to synthesize MOF platforms allow experiments to test structure-function relationships for transforming CO$_2$ into useful chemicals. Herein, recent developments are highlighted for MOFs participating as catalysts for the chemical fixation and photochemical reduction of CO$_2$. Finally, opportunities and challenges facing MOF catalysts are discussed in this ongoing research area.

1. Introduction

The world population is rapidly increasing and its inhabitants are using fossil fuels such as coal and natural gas to satisfy their energy demands. This necessity releases large amounts of carbon dioxide into the atmosphere every year. Some of this CO_2 is absorbed by oceans and seas causing a rise in seawater acidity; whereas, plants use CO_2 in photosynthesis to form organic molecules and oxygen. However, about half of the CO_2, as the primary source of greenhouse gas remains in the atmosphere, which further triggers a series of global environmental and energy problems. In the 21st century, carbon capture and storage/sequestration (CCS) is considered the most promising strategy to overcome these issues and make a significant impact in environmental protection and sustainable development.[1] Extensive efforts have been devoted to the development of heterogeneous catalysts, including metal oxides,[2] activated carbons,[3] zeolites,[4] silica-supported salts,[5] and porous polymers,[6] to use CO_2 as a chemical reagent for renewable chemical products. However, many factors limit their practical industrial applications including their energy-cost, low-efficiency, short lifetime and poor recyclability. In addition, these catalytic materials require many complicated steps to separate and purify the desired chemical product from the catalyst. Consequently, there is an urgent need to develop and examine high-efficient catalysts to capture and convert CO_2 into useful chemicals.

Metal-organic frameworks (MOFs) heightened popularity for porous material applications in chemistry and materials science during recent decades come from their structural diversity,[7] and far reaching applications including gas separation,[8] drug delivery,[9] sensing,[10] catalysis,[11] and proton conductivity.[12] Many studies have demonstrated that porous MOFs performed significantly better in comparison with traditional porous materials for various applications. These investigations were mainly ascribed to the MOFs accessible high surface areas, tunable pores, and versatile chemical functionalities. MOFs are given these properties from their building components consisting of metal ions/clusters and multitopic organic ligands. A powerful driving force behind the unprecedented expansion in MOF materials is that a desired framework topology platform and chemical recognition sites can be targeted by the judicious selection of metal clusters and organic linkers.[13]

Heterogeneous catalysis is becoming one of the most active domains in MOF research. MOFs feature a large number of catalytic sites from both metal clusters and organic ligands. The open metal sites always serve as Lewis acid sites and are situated on inorganic clusters or organometallic linkers (e.g., metalloporphyrins and metallosalens). The pores size (cavities and windows) and chemical environment can be controlled from the framework components resulting in a size and supramolecular selective catalyst. Furthermore, MOFs have displayed several other significant properties such as high CO_2 adsorption uptake which can enhance the local concentration of CO_2 around the catalytic active centers inside the pores of the framework to improve catalytic efficiency. Indeed, the framework pores are able to enclose CO_2 within a "nanoreactor" environment for its transformation. Furthermore, MOFs separate easily from liquid or gas phase reactions allowing for simple recycling.

The method used to transform CO_2 into different products is quantified in multiple ways. Using a homogeneous catalyst, the rate law, Equation (1), can be applied as demonstrated by North and Pasquale.[14] In photochemical reactions where CO_2 is reduced into different products the quantum yield (ϕ), Equation (2), can determine the efficiency with the incoming photons. For other reactions, the turnover number (TON) is calculated as the molar ratio of CO_2 products to the catalyst concentration, Equation (3).[15]

$$\text{Rate} = k\,(\text{epoxide})^1\,(\text{CO}_2)^1\,(\text{catalyst})^1\,(\text{co}-\text{catalyst})^2 \qquad (1)$$

$$\phi = (\text{CO}_2 \text{ reduction products}) / (\text{incident photons}) \qquad (2)$$

$$\text{TON} = (\text{CO}_2 \text{ products}) / (\text{catalyst}) \qquad (3)$$

This review highlights recent scientific contributions to the chemical transformation of CO_2 using MOFs as heterogeneous catalysts and separates reactions into three main categories. First, chemical fixation of CO_2 with epoxides to synthesize cyclic organic carbonates; second, electrocatalytic or photochemical reduction of CO_2 using MOFs or its composites/hybrids to generate renewables; and finally, CO_2 carboxylation onto MOF ligands or terminal alkynes. This review provides an overview and inspiring perspectives of MOFs as heterogeneous catalysts for CO_2 chemical transformations.

2. Chemical Fixation of CO_2 with Epoxides into Cyclic Organic Carbonates

Cycloaddition reactions between CO_2 and epoxides are some of the most efficient approaches to convert CO_2 into valuable chemicals.[16] These reactions produce cyclic organic carbonates which are widely used in the pharmaceutical and chemical industries. Therefore, extensive research studies have been focused on the development of heterogeneous catalysts for cycloaddition reactions. Notably, MOFs can possess open metal centers that participate as Lewis acid sites in order to

H. He, Dr. J. A. Perman, Prof. S. Ma
Department of Chemistry
University of South Florida
4202 East Fowler Avenue
Tampa, Florida 33620, USA
E-mail: sqma@usf.edu

H. He, Prof. G. Zhu
State Key Laboratory of Inorganic Synthesis
and Preparative Chemistry
College of Chemistry
Jilin University
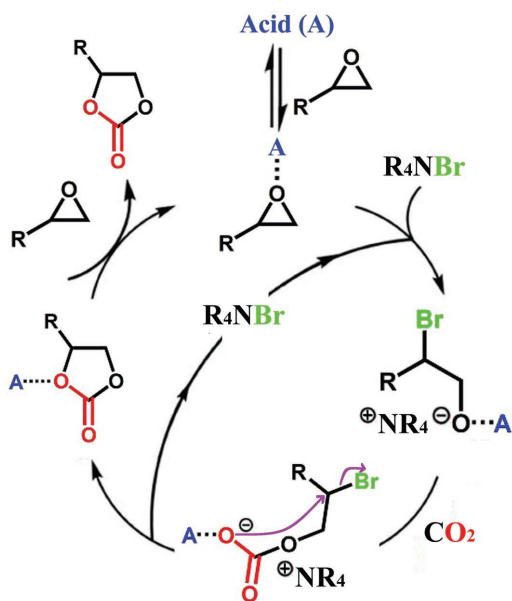Changchun 130012, China
E-mail: zhugs@jlu.edu.cn

Figure 1. Proposed mechanism for the acid (A)-catalyzed cyclic carbonate synthesis from epoxides and CO_2 in the presence of a tetraalkyl ammonium halide (bromide).

Hongming He joined the group of Prof. Honggang Fu during his B.S. research project. Then he received his bachelor's degree in Materials Chemistry from Heilongjiang University, China in 2011. In the fall of 2011, he joined the research group of Prof. Guangshan Zhu for his PhD program at Jilin University, China. He joined the research group of Prof. Shengqian Ma as a visiting student in June 2015. His current research focuses on the development of metal organic frameworks for gas storage, chemical sensor, and heterogeneous catalysis.

Jason A. Perman received his Ph.D. in Inorganic Chemistry from the University of South Florida in 2011 under the supervision of Dr. Michael J. Zaworotko. After finishing postdoctoral fellowships abroad, he returned and joined Dr. Shengqian Ma's research group in 2016. Current research interests include metal-organic materials, supramolecular chemistry, carbon capture and sequestration, and green chemistry.

Shengqian Ma received his BS degree from Jilin University, China in 2003, and graduated from Miami University (Ohio) with a PhD degree under the supervision of Hong-Cai "Joe" Zhou (currently as Texas A&M University) in 2008. After finishing two-year Director's Postdoctoral Fellowship at Argonne National Laboratory, he joined the Department of South Florida as an assistant Professor in August 2010. His current research interests focus on the development of functional porous materials for energy, biological, environmental-related application.
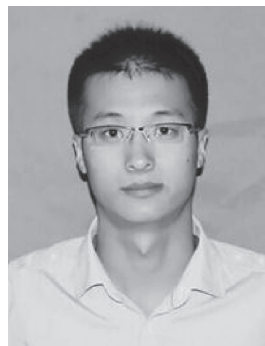
promote catalytic cycloaddition reactions. Previously, Beyzavi and colleagues reported a tentative mechanism as shown in **Figure 1**, for the cyclic carbonate synthesis in the presence of a Lewis acid.[17]

As summarized in **Table 1**, MOFs have been reported to catalyze CO_2 with the epoxides shown in **Figure 2**, under different reaction conditions. These MOFs are further categorized into four subcategories based on different catalytic sites.[18–54] The subcategories promoting catalysis include: structural defects in the MOF, open metal sites from metal clusters, tandem Lewis acid sites from the metal cluster and organometallic linker, and co-catalyst functionalized MOFs.

2.1. MOFs with Active Catalytic Defect Sites

MOFs with both saturated metal clusters and organic ligands can catalyze the cycloaddition reaction between CO_2 and epoxides at defect sites within or on the surface of the crystalline materials.[18–23] In 2009, Song and co-workers reported on MOF-5, saturated Zn_4O clusters linked by BDC ligands, to catalyze CO_2 and epoxides in the presence of a quaternary ammonium salt co-catalysts.[18] They attributed the reactivity to defects at the Zn_4O cluster sites and also discovered that the yield of propylene carbonate depended strongly on the quaternary ammonium salts. The yield of propylene carbonate increased with the alkyl chain length in the following order: n-Bu_4N^+ > n-Pr_4N^+ > Et_4N^+ > Me_4N^+. In comparison with the individual framework components H_2BDC, $ZnCl_2$, and ZnO, with n-Bu_4NBr, MOF-5/n-Bu_4NBr exhibited the highest catalytic activity, approaching 100%, under mild conditions (Table 1, Entry 1). Furthermore, the catalyst was easily separated and recycled from the reaction.

MOFs synthesized using imidazole ligands yielding crystals with zeolitic-like topologies are termed zeolitic imidazolate frameworks (ZIFs). In particular, ZIF-8 forms a porous sodalite network from the reaction between $Zn(NO_3)_2 \cdot 4H_2O$ and 2-methylimidazole, where the Zn^{2+} ions are saturated from four ligands coordinated in a tetrahedral motif. Miralda et al. reported that ZIF-8 can be used as a heterogeneous catalyst for the cycloaddition of CO_2 and epichlorohydrin to form chloropropene carbonate.[19] These reactions were carried out between 70 and 100 °C at 7 bar CO_2 for a duration of four hours. They additionally functionalized ZIF-8 with ethylene diamine, enhancing CO_2 adsorption, and showed that the catalytic yield improved at 80 °C (Table 1, Entry 2), but it dramatically had a lower yield upon the first recycling. ZIF-8 contains both Lewis acid sites from zinc ions and base sites from the imidazole nitrogen atoms, which were believed to promote catalysis at defect sites in the crystal.

Similar research by Yang and co-workers in 2014, investigated the catalytic behavior of ZIF-68 for the synthesis of

Table 1. Cycloaddition reaction of CO_2 with epoxides catalyzed by different MOFs.

Entry	Substrate	MOF	Chemical formula (guest molecule ignored)[a]	Co-catalyst	T.[b] [K]	P.[c] [atm]	Time [h]	% Yield	Ref.
1	a	MOF-5	$(Zn_4O)(BDC)_3$	n-Bu$_4$NBr	323	60	4	98	[18]
2	d	ZIF-8; NR$_2$-ZIF-8	$Zn(MeIM)_2$	–	353	7	4	44, 73	[19]
3	l	ZIF-68	$Zn(bIM)(nIM)$	–	393	10	12	93	[20]
4	a, l, n, d	ZIF-67	$Co(MeIM)_2$	–	373	10	8, 15, 14, 8	96, 92, 93, 99	[21]
5	i, d, a, l, k	ZIF-67	$Co(mIM)_2$	–	393	10	6	94, 97, 98, 73, 8	[22]
6	a	ZIF-90	$Zn(ICA)_2$	–	393	12	8	81	[23]
7	l, n, o, r	Ni-TCPE1	$Ni_2(TCPE)$	n-Bu$_4$NBr	373	10	12	>99, >99, 96, 94	[24]
8	l, n, o, r	Ni-TCPE2	$Ni_2(TCPE)$	n-Bu$_4$NBr	373	10	12	86, 98, 94, 93	[24]
9	a, c, l, d	*gea*-MOF-1	$Y_9(\mu_3\text{-}OH)_8(\mu_2\text{-}OH)_3(BTB)_6$	n-Bu$_4$NBr	393	20	6	88, 94, 85, 89	[25]
10	a	$(Zn_4O)_2(Zn_2)_{1.5}(CPD)_6$	$(Zn_4O)_2(Zn_2)_{1.5}(CPD)_6$	n-Bu$_4$NBr	r. t.[d]	12	60	99	[26]
11	a, l	Hf-NU-1000	$Hf_6(\mu_3\text{-}OH)_8(OH)_8(TBAPy)_2$	n-Bu$_4$NBr	r. t.	1	26, 56	100, 100	[27]
12	l	NU-1000	$Zr_6(\mu_3\text{-}OH)_8(OH)_8(TBAPy)_2$	n-Bu$_4$NBr	r. t.	1	56	46	[27]
13	a, b, d, c	USTC-253-TFA	$Al(OH)(SBPDC)_x(TFA)_{1-x}$	n-Bu$_4$NBr	298	1	72	81, 55, 38, 43	[28]
14	a	USTC-253	$Al(OH)(SBPDC)$	n-Bu$_4$NBr	298	1	72	74	[28]
15	a	MIL-53	$Al(OH)(BDC)$	n-Bu$_4$NBr	298	1	72	54	[28]
16	a	MOF-253	$Al(OH)(BPYDC)$	n-Bu$_4$NBr	298	1	72	82	[28]
17	a	MIL-101	$Cr_3F(H_2O)_2O(BDC)_3$	n-Bu$_4$NBr	298	1	72	31	[28]
18	a	UiO-66	$Zr_6(\mu_3\text{-}O)_4(\mu_3\text{-}OH)_4(BDC)_{12}$	n-Bu$_4$NBr	298	1	72	55	[28]
19	a	ZnGlu	ZnGlu	n-Bu$_4$NBr	r. t.	10	24	65	[29]
20	a	ZnGlu	ZnGlu	n-Bu$_4$NBr	353	12	6	>99	[30]
21	a, c, h, l	In$_2$(OH)(BTC)(HBTC)$_{0.4}$(L)$_{0.6}$	$In_2(OH)(1,2,4\text{-}BTC)(1,2,4\text{-}HBTC)_{0.4}(L)_{0.6}$	n-Bu$_4$NBr	353	20	4	94, 91, 85, 73	[31]
22	l	Mg-MOF-74	$Mg_2(DHTP)(H_2O)_2$	–	373	20	4	95	[32]
23	g, d, e, l	BIT-C	CuL_1	n-Bu$_4$NBr	333	1	6	99, 99, 95, 99	[33]
24	l, n	Ba(H$_2$TADP)$_{0.5}$	$Ba(H_2TADP)_{0.5}$	n-Bu$_4$NBr	353	6	4	80, 98	[34]
25	a, c, l, j, n	Zn$_3$(PTB)$_2$	$Zn_3(PTB)_2$	n-Bu$_4$NBr	r. t.	1	48	92, 89, 78, 70, 39	[35]
26	a, d, l, n, k	BIT-103	$Zn_3(BTC)_2$	–	433	30	24, 8, 24, 24, 24	100, 100, 97, 100, 16	[36]
27	a, d, f, l, n, l, k	Cu(HIP)$_2$(BPY)	$Cu(HIP)_2(BPY)$	–	393	12	6	62, 72, 56, 73, 71, 56, 10	[37]
28	a, c, h, i	MMPF-9	$Cu_6(Cu\text{-}TDPBPP)(HCO_2)_4(H_2O)_6$	n-Bu$_4$NBr	r. t.	1	48	87, 80, 30, 30	[38]
29	a	PCN-224(Co)	$Zr_6(\mu_3\text{-}O)_4(\mu_3\text{-}OH)_4(Co\text{-}TCPP)_3$	n-Bu$_4$NCl	373	20	4	42	[39]
30	a, c, d, i, n	MMPF-18	$Zn_4(\mu_4\text{-}O)(Zn\text{-}BCPP)_3$	n-Bu$_4$NBr	r. t.	1	48	97, 97, 99, 100, 33	[40]
31	a, d, l, m, n	Cd$_2$(Ni-BHP)$_2$	$Cd_2(Ni\text{-}BHP)_2$	n-Bu$_4$NBr	353	20	4	80, 84, 81, 76, 55	[41]
32	a, c, i, h, n	MMCF-2	$Cu_2(Cu\text{-}TACTMB)(H_2O)_3(NO_3)_2$	n-Bu$_4$NBr	r. t.	1	48	95, 89, 43, 42, 38	[42]
33	a	HKUST-1	$Cu_3(BTC)_2$	n-Bu$_4$NBr	r. t.	1	48	49	[42]
34	a	MOF-505	$Cu_2(BPTC)(H_2O)_2$	n-Bu$_4$NBr	r. t.	1	48	48	[42]
35	a	MIL-101-N(or P)(n-Bu)$_3$Br	$Cr_3F(H_2O)_2O(BDC)_x(F\text{-}BDC)_{3-x}$	–	353	20	8	99; 98	[43]
36	d, c, l	F-IRMOF-3	$(Zn_4O)(BDC\text{-}NH_2)_x(F\text{-}BDC)_{3-x}$	–	413	20	1.5, 2, 5	80, 90, 84	[44]
37	i	F-ZIF-90	$Zn(ICA)_x(F\text{-}ICA)_{2-x}$	–	393	11.7	6	97	[45]
38	a, d, i, l, k	IL-ZIF-90	$Zn(ICA)_x(IL\text{-}ICA)_{2-x}$	–	393	10	3	97, 94, 94, 81, 9	[46]
39	l	MIL-68(In)	$In(OH)(BDC)$	–	423	8	8	39	[47]
40	l	MIL-68(In)-NH$_2$	$In(OH)(BDC\text{-}NH_2)$	–	423	8	8	71	[47]
41	l	UiO-66-NH$_2$	$Zr_6(\mu_3\text{-}O)_4(\mu_3\text{-}OH)_4(BDC\text{-}NH_2)_{12}$	–	373	20	1, 4	70, 95	[48]
42	l	UiO-66	$Zr_6(\mu_3\text{-}O)_4(\mu_3\text{-}OH)_4(BDC\text{-}NH_2)_{12}$	–	373	20	1, 4	48, 94	[48]
43	a, d, I, l, k	UMCM-1-NH$_2$	$(Zn_4O)_9(BDC\text{-}NH_2)_6(BTB)_5$	n-Bu$_4$NBr	r. t.	12	24	90, 78, 85, 53, 10	[49]
44	a, c, d, e	Cu$_4$MTTP	Cu_4MTTP	n-Bu$_4$NBr	r. t.	1	48	96, 83, 85, 88	[50]

Table 1. Continued

Entry	Substrate	MOF	Chemical formula (guest molecule ignored)[a]	Co-catalyst	T.[b] [K]	P.[c] [atm]	Time [h]	% Yield	Ref.
45	a	$Zn_4O(BDC)_x(BDC\text{-}NH_2)_{3-x}$	$Zn_4O(BDC)_x(BDC\text{-}NH_2)_{3-x}$	Et_4NBr	413	40	3	63	[51]
46	l, n, f, g, k	UiO-66-NH$_2$(gel)	$Zr_6(\mu_3\text{-}O)_4(\mu_3\text{-}OH)_4(BDC\text{-}NH_2)_{12}$	n-Bu$_4$NBr	373	1	8, 4, 4, 5, 6	91, 92, 99, 99, 28	[52]
47	a	$Zn(L_2)R$ (R = IP;HIP;AIP;NIP;HBTC)	$Zn(L_2)R$ (R = IP;HIP;AIP;NIP;HBTC)	–	373	30	6	54; 40; 92; 53; 37	[53]
48	a, d, c, l, n, q	$Zn_6(TATAB)_4(DABCO)_3$	$Zn_6(TATAB)_4(DABCO)_3$	–	373	1	16	100, 98, 92, 90, 85, 8	[54]

[a]Ligands are abbreviated as: H_4TCPE = Tetrakis(4-carboxyphenyl)ethylene; Glu = L-glutamic acid; H_4TBAPy = 1,3,6,8-tetrakis(p-benzoic acid)pyrene; H_2SBPDC = 4,4′-dibenzoic acid-2,2′-sulfone; TFA = Trifluoroacetic acid; H_2BDC = Benzene-1,4-dicarboxylate; H_2BPYDC = 2,2′-bipyridine-5,5′-dicarboxylate acid; HMeIM = 2-methylimidazolate; H_3CPD = 10-(4-carboxy-phenyl)-10H-phenoxazine-3,6-di-carboxylic acid; H_3BTB = 1,3,5-tri(4-carboxyphenyl)benzene; H_4bcpp = 5,15-bis(4-carboxyphenyl)porphyrin; 1,2,4-H_3BTC = 1,2,4-benzenetricarboxylic acid; L_1 = (Z)-2-(5-chlorin-2-hydroxy benzylideneamino) acetic acid; H_4TADP = 5,5′-(2,3,6,7-tetramethoxyanthracene-9,10-diyl)diisophthalic acid; H_3PTB = 4,4′,4″-(pyridine-2,4,6-triyl(tribenzoic acid); H_6TDCBPP = Tetrakis(3,5-dicarboxybiphenyl)-porphine; H_4TACTMB = 1,4,7,10-tetrazazcyclododecane-N,N′,N″,N‴-tetra-p-methyl-benzoic acid; H_3BTC = 1,3,5-benzenetricarboxylic acid; H_4BPTC = 3,3′,5,5′-biphenyltetracarboxylate; H_4BHP = (E)-3-(3-tert-butyl-5-fomyl-4-hydroxyphenyl)acrylic acid; H_6TCPP = Tetrakis(4-carboxyphenyl)-porphyrin; H_2BDC-NH$_2$ = 2-aminobenzene-1,4-dicarboxylate; H_8MTTP = 5,5′,5″,5‴-((methanetetrayltetrakis-(benzene-4,1-diyl)tetrakis(1H-1,2,3-triazole-4,1-diyl))tetraiso-phthalic acid; HICA = Imidazolate-2-carboxaldehyde; HbIM = Benzimidazole; HnIM = 2-nitroimidazole; H_4DHTP = 2,5-dihydroxybenzene carboxylic acid; L_2 = $N^4,N^{4'}$-di(pyridine-4-yl)biphenyl-4,4′-dicarboxamide; H_2IP = isophthalic acid; H_2HIP = 5-hydroxy-isophthalic acid; H_2AIP = 5-amino-isophthalic acid; H_2NIP = 5-nitroisophthalic acid; H_3TATAB = 4,4′,4″-s-triazine-1,3,5-triyl-tri-p-aminobenzoic acid; DABCO = 1,4-diazabicyclo[2.2.2]octane; BPY = 4,4′-bipyridine; [b]T. = temperature; [c]P. = pressure; [d]r. t. = room temperature.

styrene carbonate from CO_2 and styrene oxide.[20] ZIF-68 is composed of 2-nitroimidazole and benzimidazole linked with Zn^{2+} cations to give it a gme topology (gmelinite) containing two large pores with diameters of 7.5 and 10.3 Å (**Figure 3**). The ZIF-68 demonstrated remarkable catalytic activity for the CO_2 cyclic addition reactions, which were conducted between 80 and 130°C at pressures between 2 and 30 bar CO_2 for a duration of 12 hours (Table 1, Entry 3). Notably, the catalytic performance of ZIF-8 showed lower activity than ZIF-68 when investigated under the same condition because larger pores in ZIF-68 held higher amounts of CO_2. They also evaluated the acid and base sites within ZIF-68 using NH_3 and CO_2 temperature-programmed desorption experiments and discovered defect sites in the structure, including unsaturated coordinative Zn^{2+} cations participating as Lewis acid sites and exposed nitrogen atoms from 2-nitroimidazole or benzimidazole ligands participating as base sites. In addition, ZIF-68 was recycled a further three times after the initial catalysis showing its excellent chemical and thermal stability under these conditions. These MOF catalysts required high temperature and pressure conditions for the cycloaddition reaction and this process may not be preferred when applied on a larger scale. Hence, it is a challenge to develop MOFs

catalysts to promote this reaction under milder reaction conditions.

2.2. MOFs with Active Catalytic Metal Sites

Representative studies for the chemical transformation of CO_2 with epoxides into cyclic organic carbonates using MOFs with unsaturated metal cations are reviewed.[24–37] The accessible and unsaturated metal cations function as Lewis acid sites to activate the epoxide substrates, but these reactions require a co-catalyst such as a Lewis base to open the epoxide ring. It is worth noting that these metal clusters are multinuclear complexes rather than mononuclear species, resulting in additional factors that influence their catalytic activities.

Zhou and colleagues reported a porous MOF resembling open nanotubes as a heterogeneous catalyst for the cycloaddition reactions involving CO_2.[24] From the single crystal structure of Ni-TCPE1 (**Figure 4**a–d), Ni^{2+} cations are exposed on the inner tubular surface to participate as the Lewis acid sites. It was found that the organic substrates can penetrate deeply into the open channels rather than on the surface as measured by confocal laser scanning microscopy of guest dye molecules adsorbed in the crystals. Ni-TCPE1 showed a maximum CO_2 capacity of 48 and 33 cm^3 g^{-1} at 273 and 298 K, respectively. Experiments were performed in a high pressure reactor containing the epoxide (20 mmol), catalyst (10 μmol, based on Ni), and n-Bu$_4$NBr (0.3 mmol) with CO_2 (10 bar) for a duration of 12 hours at 100°C. Nearly quantitative conversion of the starting materials, styrene oxide or 2-(phenoxymethyl)-oxirane, were converted to their corresponding carbonates (Table 1, Entries 7
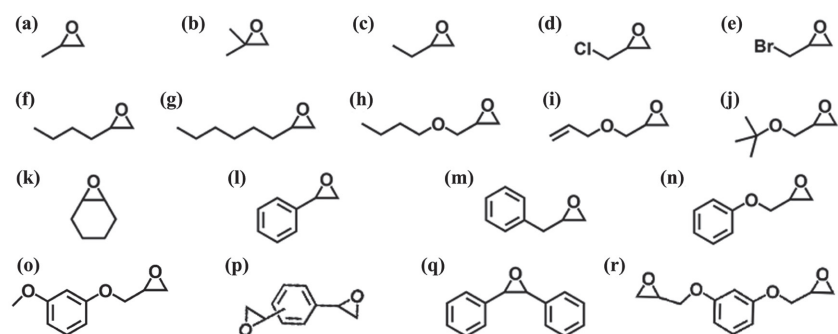

Figure 2. Epoxides used for the cycloaddition reaction of CO_2 catalyzed by MOFs in this review.
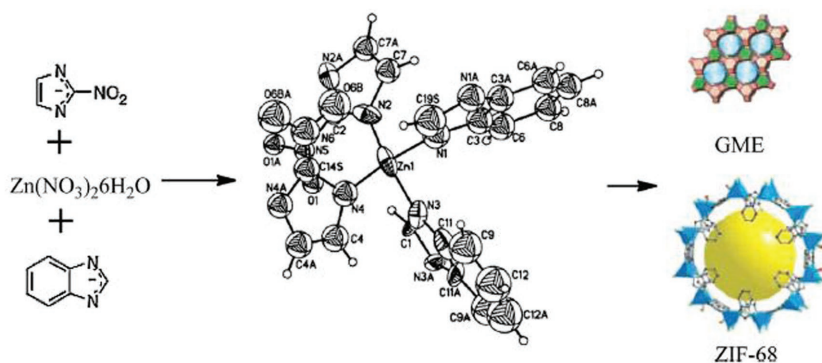
Figure 3. Synthesis and topology structure of ZIF-68: the largest cage is shown with ZnN_4 tetrahedral in blue, the inside yellow ball in the structure indicates space in the cage clearly. Reproduced with permission.[20] Copyright 2014, Elsevier.

and 8). When oxiran-2-ylmethoxy or methoxy groups were introduced into the phenyl ring of the epoxide molecule, the corresponding product yields were 96% and 94% under the same reaction conditions, respectively. CO_2 cycloaddition reactions with *R*- or *S*-styrene oxide showed outstanding enantioselectivity with an *ee* value of 92%. X-ray structural analysis of the styrene-oxide-impregnated crystals revealed that the phenyl groups of the TCPE ligands and those of the substrates showed aromatic edge-to-face interactions with the shortest distance at 3.43 Å (Figure 4e and f). Additional information from IR and ^1H NMR spectra also demonstrated that the substrate can enter the channels of Ni-TCPE1 (Ni-TCPE1′). Another catalyst Ni-TCPE2 was successfully synthesized using similar reaction conditions, besides the amount of L-proline. Ni-TCPE2 showed efficient catalytic activity to the cycloaddition of CO_2 and epoxides. However, the catalytic efficiency of Ni-TCPE2 is lower than that of Ni-TCPE1, which was ascribed to weaker interactions between the substrate and the MOF, and pore blockage from an unknown carbonaceous material formed during the MOF synthesis.
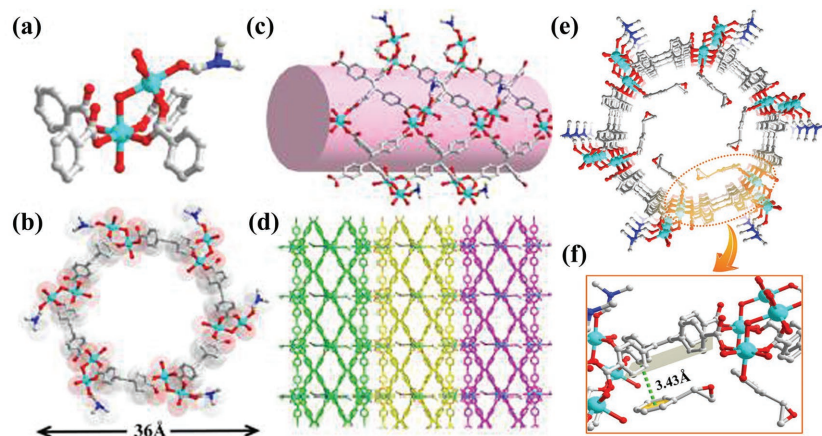
In 2014, Guillerm and co-workers used an 18-connected yttrium cluster ($Y_9(\mu_3$-$OH)_8(\mu_2$-$OH)_3(O_2C$-$)_{18})^{2-}$ to prepare a MOF with gea topology (gea-MOF-1).[25] It was synthesized in a solvothermal reaction between 1,3,5-benzene(tris)benzoate (H_3BTB), 2-fluorobenzoic acid, and $Y(NO_3)_3•6H_2O$ in a DMF/water solution. Single crystal X-ray diffraction analysis revealed that the anionic yttrium cluster is an 18-connected node linked to 18 triangular BTB ligands to obtain a three-dimensional porous framework (**Figure 5**). Due to its high stability, large porosity, and high surface area, gea-MOF-1 was evaluated as a heterogeneous catalyst for cycloaddition reactions. A mixture of the substrate (100 mmol), gea-MOF-1 (60 mg, equaling 0.15 mmol yttrium), *n*-Bu_4NBr (0.15 mmol), and CO_2 (20 bar) was heated at 120°C for six hours under a solvent-free environment (Table 1, Entry 9). The conversion of CO_2 and propylene oxide to propylene carbonate was 88% and remained high at 77% after the third recycling. However, lower turnover frequency was observed for gea-MOF-1 than the homogeneous YCl_3/*n*-Bu_4NBr, due to mass-transport limitations and less Lewis acid (Y^{3+}) sites in the MOF. For comparison, the catalytic reaction in gea-MOF-1 was better than the heterogeneous catalyst Y_2O_3/*n*-Bu_4NBr, demonstrating that accessible Lewis acid (Y^{3+}) sites and larger surface area play important roles in the reaction.

In 2016, Zou and the co-workers reported a highly porous MOF, called 1-Zn, with a BET surface area of 2969 m^2 g^{-1} and accessible Lewis acid sites suitable for catalyzing the cycloaddition reactions.[26] Two types of metal clusters, the dimeric paddlewheel ($Zn_2(COO)_4$) and tetrameric ($Zn_4(\mu_4$-$O)$ $(COO_2)_6$), are present in the structure and can undergo metal ion exchange. Interestingly, Cu^{2+} and Co^{2+} ions can be introduced into the dimeric paddlewheel ($Zn_2(COO)_4$) via single-crystal-to-single-crystal exchange to obtain 1-Cu and 1-Co, which can provide a novel platform to study how the metal effects the catalytic performance (**Figure 6**a). In a typical reaction, Zou et al. mixed together propylene oxide (40 mmol), *n*-Bu_4NBr (1.5 mmol, 3.75 mol%), and their MOF (0.0064 mmol, 0.016 mol% based on paddle-wheel units) in a Parr reactor vessel under 12 bar CO_2 for 60 hours at room temperature. They achieved yields of propylene carbonate at 99%, 32%, and 50% for 1-Zn, 1-Cu, and 1-Co, respectively (Table 1, Entry 10). It was reasoned that the high catalytic efficiency of 1-Zn for this reaction may be due to the lower energy gap between the HOMO of epoxy propane and LUMO of CO_2 on the open metal active sites, and the higher binding energy of CO_2 to the metal centers as described

Figure 4. a) Structure of Ni-TCPE1 exhibiting the binuclear Ni_2 unit. b) The top view of nanotube. c) The side view of 1D nanotube with the pink column representing the channel. d) The packing pattern between them along the *b* axis. e) The structure of styrene oxide impregnated Ni-TCPE1′. f) Enlarged view of the Ni-TCPE1′ exhibiting the positions of the substrate and the interactions between the tube and the substrate. Color code: Ni, cyan; O, red; N, blue; C, gray. The hydrogen atoms and lattice solvents are omitted for clarity. Reproduced with permission.[24] Copyright 2015, American Chemical Society.

(a)

Cavity I   Cavity II

Cavity III   gea-MOF-1
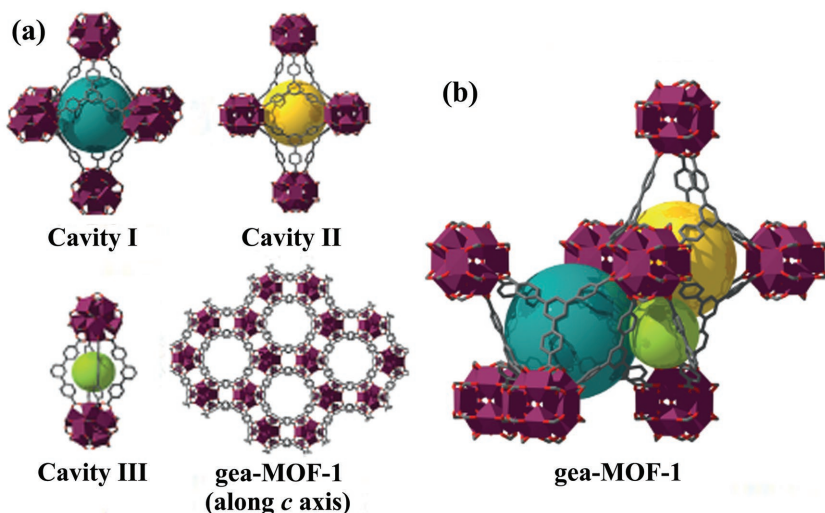(along *c* axis)

(b)

gea-MOF-1

Figure 5. a) Structural representations of *gea*-MOF-1 with three types of cavity. b) The packing of these cavities in gea-MOF-1. The hydrogen atoms are omitted for clarity. Color code: Re, purple; C, grey; O, red. Reproduced with permission.[25] Copyright 2014, Nature Publishing Group.

co-catalyst role did show its importance in these reactions. Therefore the next challenge will be to design MOFs that don't require co-catalysts.

2.3. MOFs with Dual Catalytic Metal Centers

Lewis acid sites on the metal clusters encouraged researchers to include another on the ligand (organometallic ligand), thus increasing the concentration of catalytic sites within a MOF.[38–42] Metalloporphyrins as ligands in MOF served as the catalytic sites for the CO_2 fixation reaction.[38–40] Recently, Gao and co-workers explored a metalloporphyrin-based MOF, named MMPF-9, for heterogeneous catalysis in CO_2 fixation reactions.[38] Dark red block-shaped crystals of MMPF-9 were synthesized from $Cu(NO_3)_2 \cdot 2.5H_2O$ and the porphyrin

by molecular dynamic simulations (Figure 6c). Furthermore, these MOFs are recyclable as they retained their pristine structures and activities after three successive catalytic reactions (Figure 6b). Although defects are likely present in the preceding MOFs which exhibited high catalytic yields, the

$H_{10}TDCBPP$ under solvothermal conditions. The porphyrin macrocycles were metallated with Cu^{2+} during the synthesis. As shown in **Figure 7**, MMPF-9 has two channels: (*a*) a truncated triangle channel with an aperture of 14.0 Å surrounded by three TDCBPP(Cu) ligands and six copper paddlewheel
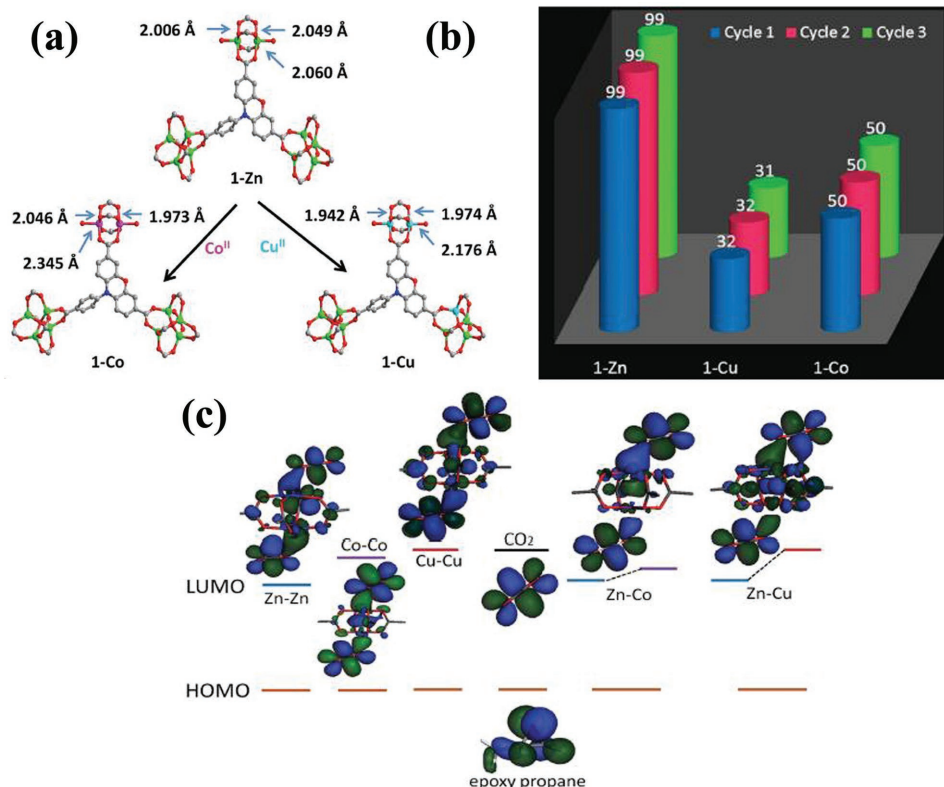

Figure 6. a) The fragmental cluster change via metal cation exchange in 1-Zn. The hydrogen atoms are omitted for clarity. Atom color: Zn (green), Cu (blue), and Co (pink). b) The propylene carbonate yields of the cycloaddition of CO_2 and propylene oxide with different MOF catalysts up to three cycles. c) LUMO orbital of CO_2 adsorbed on different metal centers of MOFs during the catalytic process. Reproduced with permission.[26] Copyright 2016, Wiley-VCH.
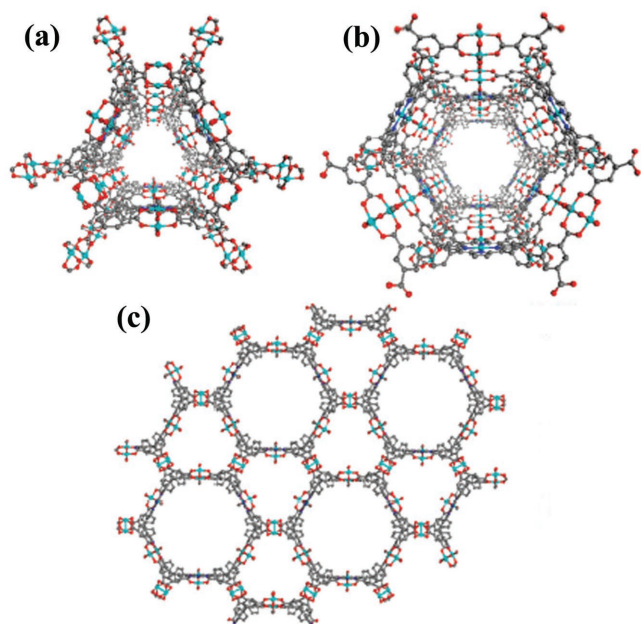
Figure 7. a) The truncated trigular channel. b) The hexagonal channel and c) the extended channels of MMPF-9 viewed along the *c* direction. Reproduced with permission.[38] Copyright 2014, Royal Society of Chemistry.

clusters, and (*b*) a hexagonal channel with a 24.7 Å aperture surrounded by nine copper paddlewheel clusters (Table 1, Entry 28). The high density of copper sites in MMPF-9 exhibited excellent catalytic performance for cycloaddition of propylene oxides using CO_2 to generate propylene carbonate under 1 atm CO_2 at room temperature after 48 hours. MMPF-9 showed significantly higher catalytic activity than HKUST-1, a benchmark copper paddlewheel MOF. In addition, other metalloporphyrin MOFs, PCN-224(Co)[39] and MMPF-18,[40] showed outstanding catalytic properties.

Metallosalen molecules as ligands used in MOFs offer a second Lewis acid catalytic site, apart from the metal cluster, that may enhance the performance of the heterogeneous catalyst. Yan and co-workers used a dicarboxyl functionalized nickel salphen complex (Ni-H$_2$L) organometallic ligand assembled with Cd^{2+} ions to form brown crystals of their complex 1 [Cd$_2$(Ni-L)$_2$(H$_2$O)$_4$]•3H$_2$O.[41] As show in **Figure 8**,

there are two different types of binuclear Cd$_2$ clusters in the structure. Each cluster has four coordinated water molecules, which can be replaced by the epoxide oxygen atom for activation during cycloaddition reactions. The coordinatively unsaturated Ni^{2+} ions in the ligand enable a second site for activation. Their complex 1 was evaluated for the conversion of propylene oxide from 80 to 100 °C at 20 bar CO_2 and resulted in an 85% product yield after four hours at 100 °C. The highest yield for epichlorohydrin conversion was 84% in the presence of 1 mol% *n*-Bu$_4$NBr at 80 °C after four hours (Table 1, Entry 31). Control experiments were performed confirming that both the coordinatively unsaturated salphen complex (Ni-L) and the Cd^{2+} active sites assisted the cycloaddition reactions in complex 1. Thus Ni-H$_2$L and Cd(BPDC) were carried out separately under similar condition and showed lower yields than their complex 1. These results clearly illustrated that both metal sites can catalyze the epoxides synergistically with good catalytic efficiency.

Additional examples reported by Gao and co-workers used an NbO (niobium oxide like topology) MOF, namely MMCF-2, with dual Lewis acid catalytic metal sites, which was constructed from copper-paddlewheel clusters and the metallated azamacrocycle ligand (Cu-TACTMB).[42] MMCF-2 possessed a cuboctahedral cage with 12 copper-paddlewheel clusters on the vertexes and six Cu^{2+} metallated azamacrocycle as square faces. With a high and centralized density of Cu^{2+} centers (18 Cu^{2+} centers in each cuboctahedral cage) in the framework (**Figure 9**b and d), MMCF-2 can be used as a nanoreactor to promote the cycloaddition of CO_2 and epoxides under mild condition. MMCF-2 exhibited significantly efficient catalytic activity for cycloaddition of propylene oxide with CO_2 into propylene carbonate at room temperature and 1 atm CO_2 (Table 1, Entries 32–34). MOF-505 had the same topology as MMCF-2, but it only possessed 12 clusters in its cuboctahedral cage (Figure 9a and c). Additional experiments were carried out under the same conditions to investigate the relation between open metal centers and the catalytic properties. As shown in Figure 9e, it was found that MMCF-2 (95.4% yield) outperformed homogeneous Cu(TACTMB) (47.5% yield), MOF-505 (48% yield) and HKUST-1 (49.2% yield) for the reaction between propylene oxide and CO_2. These results indicated that the additional Cu^{2+} centers in the six square faces of
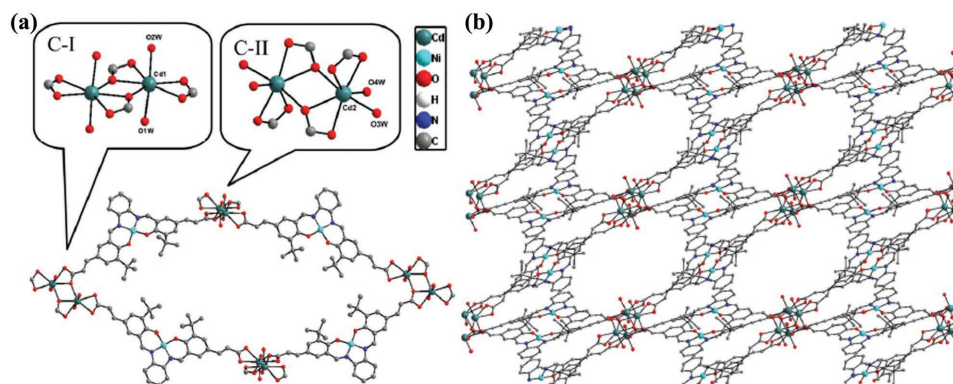

Figure 8. a) Building blocks of 1 and b) view of 3D porous structure of 1 along the *b*-axis.[41] Copyright 2013, Royal Society of Chemistry.
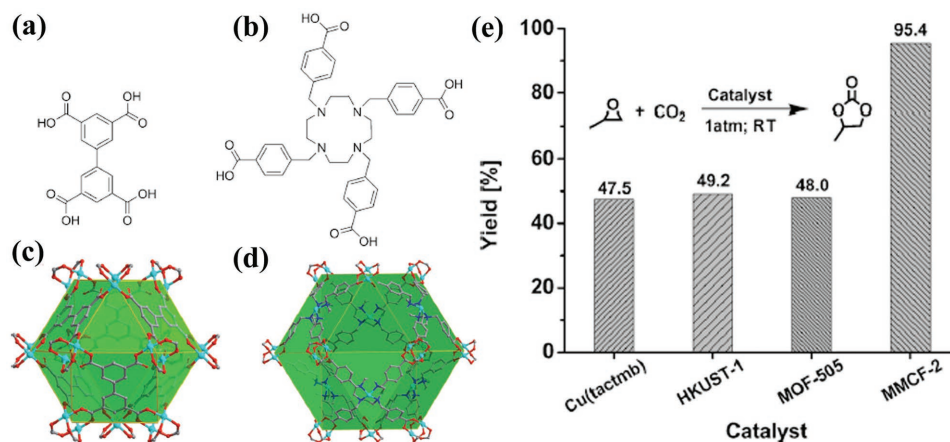
Figure 9. a) 3,3′,5,5′-biphenyltetraboxylic acid (H$_4$bptc) ligand in MOF-505; b) 1,4,7,10-tetrazazcyclododecane-*N,N′,N″,N‴*-tetra-*p*-methyl-benzoic acid (H$_4$TACTMB) ligand in MMCF-2. The cuboctahedral cage of c) MOF-505 and d) MMCF-2. e) The yield of propylene carbonate from cycloaddition of propylene oxide and CO$_2$ catalyzed by Cu(TACTMB), HKUST-1, MOF-505, and MMCF-2 after 48 h at room temperature under 1 atm CO$_2$ pressure. Reproduced with permission.[42] Copyright 2014, Wiley-VCH.

the cage significantly improve the catalytic performance via increasing the interactions between the catalytic sites and substrates. Increasing the sizes of different analytes resulted in decreased yields, which was mainly attributed to limited diffusion of larger molecules into the octahedral cage. These results suggested that if the analyte enters the cavity then the catalytic performance will improve as there are more chances to interact with the accessible Lewis acid sites. As described above, MOFs with dual catalytic metal centers can increase the concentration of catalytic sites for CO$_2$ fixation reaction. They can catalyze this reaction with higher yields under milder reaction conditions, but they required longer reaction time and a co-catalyst.

2.4. MOFs with Functional Linkers

As discussed before, the cycloaddition reaction between CO$_2$ and epoxides require metal centers as catalytic sites, but they used co-catalysts such as tetraalkyl ammonium halides in many of these reactions. As illustrated in Figure 1, the co-catalyst participates significantly to assist the epoxide change into a halo-alkoxide during the reaction. Notably, it is also found that Lewis acid sites and the co-catalyst were able to synergistically activate the intramolecular reaction. In retrospect, MOFs should be designed to incorporate Lewis acid sites from the metal clusters and co-catalysts organic molecules as ligands to produce dual functional MOFs useful at synergizing the CO$_2$ fixation reaction. Ionic liquid (IL) functional sites (*e.g.*, quaternary ammonium salts) are introduced as guests within the MOFs forming a bifunctional heterogeneous catalysts with highly efficient catalytic activity for CO$_2$ fixation. Otherwise, Lewis base functional groups (e.g., amine groups) are introduced as organic ligands, which can coordinate with metal clusters modifying the MOF with acid-base pairs. Research has shown that the acid-base pairs can effectively catalyze CO$_2$ because

carbonates formed on the base sites can react with the epoxides on the adjacent Lewis acid sites. As shown in **Figure 10**, Beyzavi et al. tentatively proposed a mechanism for forming cyclic carbonate using a Lewis acid (A) and Lewis base (B) pair in close proximity.[17]

MOFs successfully functionalized by ionic liquids include IR-MOF-3, ZIF-90, and MIL-101.[43–46] For instance, Ma and co-workers prepared two MOFs functionalized by quaternary ammonium or phosphorus bromide ionic liquid, MIL-101-N(*n*-Bu)$_3$Br and MIL-101-P(*n*-Bu)$_3$Br, by post-synthetic modification on the parent MIL-101-NO$_2$ (**Figure 11**a).[43] These bifunctional heterogeneous catalysts exhibited good catalytic performance for the CO$_2$ cycloaddition reaction under mild and co-catalyst free condition. This is mainly attributed to the synergetic effect of containing both Lewis acid sites and Br$^-$ ions from IL functionalization. Control trials were performed to synthesize propylene carbonate for some benchmark MOFs under the same condition as the modified MIL-101. As shown in Figure 11b, the bifunctional catalysts MIL-101-N(*n*-Bu)$_3$Br and MIL-101-P(*n*-Bu)$_3$Br out-performed unfunctionalized MOFs (Table 1, Entry 35). The yields of MIL-101-N(*n*-Bu)$_3$Br and MIL-101-P(*n*-Bu)$_3$Br approached 100%, higher than 2.5% for MOF-5, 5.2% for IR-MOF-3, 5.4% for HKUST, 20.9% for MIF-101, and 23.2% for Mg-MOF-74. Higher catalytic efficiency under mild reactions conditions from MIL-101-N(*n*-Bu)$_3$Br and MIL-101-P(*n*-Bu)$_3$Br was attributed to the synergetic effect between Cr^{3+} cations (Lewis acid sites) and Br$^-$ anions (co-catalysts) interacting with substrates.

Besides using the post-synthetic modification techniques, various functional groups (e.g., -NH$_2$ and -NH-) acting as
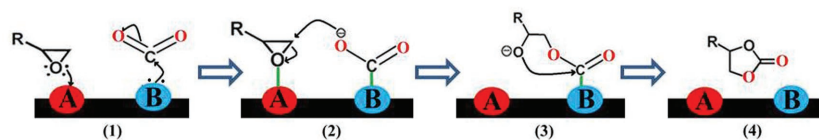

Figure 10. The proposed mechanism for catalysts with both a Lewis acid (LA) and Lewis basic (LB) pair catalyzing cyclic carbonate from epoxides and CO$_2$. Reproduced with permission.[17]
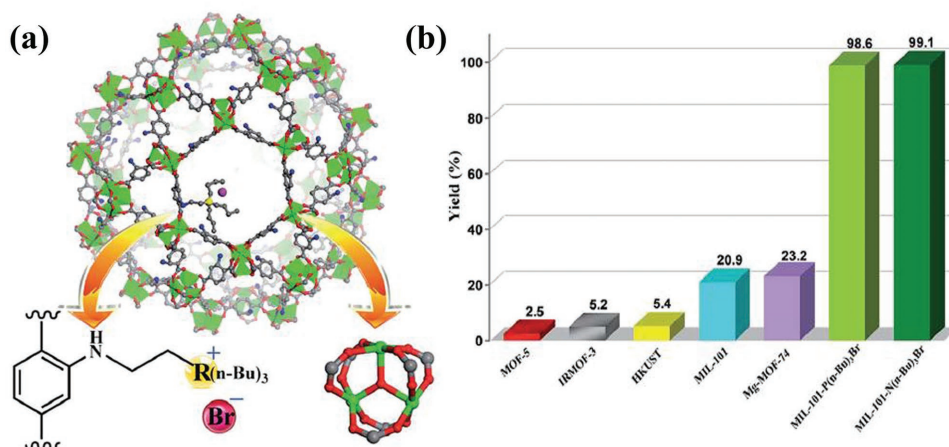
Figure 11. a) The structures of the heterogeneous catalysts: MIL-101-N(n-Bu)$_3$Br and MIL-101-P(n-Bu)$_3$Br. Atom color: Cr (green), C (gray), O (red), N (blue), Br (amaranth), and R = N or P). b) The yield of propylene carbonate from the cycloaddition of propylene oxide and CO_2 catalyzed by different MOF catalysts.[43] Copyright 2015, Royal Society of Chemistry.

Lewis base sites can be introduced in predesigned functionalized organic ligands to synthesize functional MOF catalysts with acid-base pairs. The MOFs with acid-base pairs generally exhibited better catalytic performance even without a co-catalyst.[47–54] For example, Lescouet and co-workers illuminated the vital role of an amine-functionalized MIL-68(In)-NH$_2$ for the cycloaddition reaction.[47] MIL-68(In)-NH$_2$ acid-base pairs come from the indium clusters and the amino-terephthalate ligand. The amine-functionalized MIL-68(In)-NH$_2$ exhibited higher catalytic activity than that of MIL-68(In) in the synthesis of styrene carbonate from styrene oxide and CO_2. The yields of styrene carbonate were 71% and 39% for MIL-68(In)-NH$_2$ and MIL-68(In) at 150 °C and 8 bar CO_2 for 8 h, respectively (Table 1, Entries 39 and 40). UiO-66-NH$_2$ also showed higher catalytic performance than the original UiO-66 with a styrene oxide conversion of 70% and 48%, respectively under 8 bar CO_2 pressure heated at 100 °C for one hour (Table 1, Entry 41). In addition, the efficiency of UiO-66-NH$_2$ as a catalyst was the highest among reported MOFs including UiO-66, Mg-MOF-74, MIL-101, HKUST-1, IRMOF-3, ZIF-8, and MOF-5.[48] It can be summarized that MOFs with acid-base pairs can enhance catalytic activity by introducing basic sites in the framework.

Based on the above discussion, MOFs exhibit high catalytic performance and show serious potential application for the CO_2 fixation reaction. However, many issues to commercialize these materials for large scale use in industry must be addressed such as milder reaction conditions and the co-catalyst role. Theoretical investigations should eventually provide more mechanistic details into these reactions and quickly screen for better material candidates.

3. Electrocatalytic or Photochemical Reduction of CO_2

Recently, a great deal of research efforts focused on sunlight-driven electrocatalytic or photocatalytic CO_2 reduction reactions have inspired scientist to produce numerous useful

chemicals such as CO, CH$_4$, HCOOH, and CH$_3$OH from CO_2.[55] Electrocatalytic or photochemical reduction of CO_2 becomes an ideal approach at decreasing its atmospheric concentrations and address its economic value. However, a tremendous challenges remain for CO_2 reduction catalysis because CO_2 is an extremely stable form of carbon.[56] Hence, many efforts have been devoted to the development of highly efficient catalysts for CO_2 reduction. A few MOFs have been used as electrocatalytic materials to reduce CO_2,[57–61] which were mainly attributed to their high electronic conductivities.[62] Furthermore, compared to the traditional catalysts (e.g., semiconducting materials[63] and noble metal complexes[64]), MOFs are emerging as a new class of promising photocatalysts for the effective reduction of CO_2. Currently, a series of MOFs based on Zr-, Ti-, and Fe-clusters have been applied as photocatalysts for CO_2 reduction because of their excellent chemical stability, rigid frameworks, high CO_2 uptake, broad-band visible light absorption, and efficient photoinduced charge generation. Additionally, a few hybrid materials based on MOFs were prepared and utilized for photocatalytic CO_2 reduction. This section is further organized into four categories depending on how the materials were used in CO_2 reduction reactions.

3.1. MOFs for Electrocatalytic Reduction of CO_2

A few MOFs have been investigated for CO_2 electrocatalytic reduction over the last few years[57–61] because they all have high electronic conductivities.[62] In 2012, Kumar and co-workers used uniform films of HKUST-1 as an efficient electrocatalyst for the selective reduction of CO_2 in a DMF electrolyte solution.[57] From their cyclic voltammetry experiments it was discovered that Cu$^+$ species were generated during the catalytic process. In 2015, Yaghi's group synthesized a nanosized cobalt-porphyrin MOF thin film (**Figure 12**a–c), Al$_2$(OH)$_2$TCPP-Co, which showed a selectivity for CO production in excess of 76% and a high TON of 1400 for the stable catalyst.[58] As shown in Figure 12d–f,
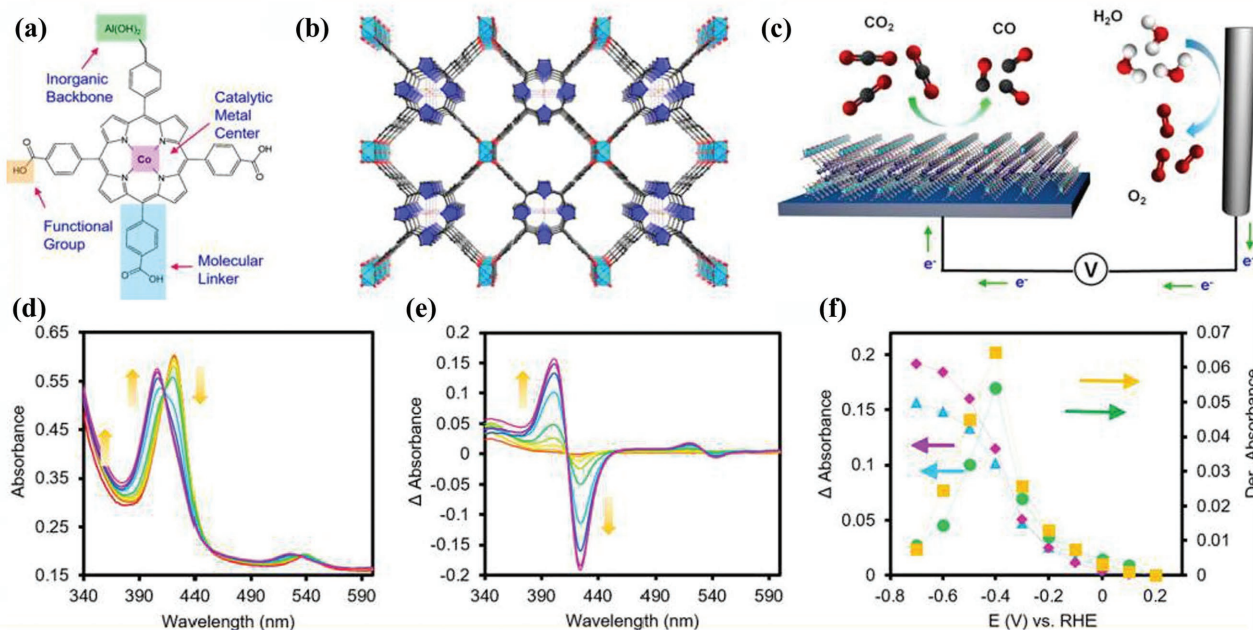
Figure 12. a) The modulation of metal centers, molecular linkers, and functional groups at the molecular level. b) The 3D structure of $Al_2(OH)_2TCPP$-Co. c) The MOF is integrated with a conductive substrate to generate a functional CO_2 electrochemical reduction system. d) The situ spectroelectrochemical demonstrate the Co(II) Scoret band decrease at 422 nm and the other Co(I) Scoret band increase at 408 nm by varying the voltage from 0.2 to −0.7 V vs RHE. e) This change is quantified and plotted to illuminate a formal redox potential of the Co catalytic center. f) It is deemed to be at the peak of the first derivative of the Co(II) bleach and Co(I) enhancement.[58] Copyright 2015, American Chemical Society.

the in situ spectroelectrochemical experiments demonstrated that the Co^{2+} Soret band intensity decreased at 422 nm and the Co^+ Soret band intensity increased at 408 nm by varying the voltage from 0.2 to −0.7 V vs RHE. This result was further confirmed by the formal redox potential of the Co catalytic center. Unfortunately, little research has been successfully preformed for electrocatalytic reduction of CO_2 and it is important for more MOF catalysts to be tested and computationally studied.

3.2. Photoactive MOF with Metal Clusters and Organic Linkers

Up to now, a few photoactive MOF photocatalysts have been reported, including Zr-MOFs,[65–69] Fe-MOFs,[70] and Ti-MOFs.[71] The catalytic centers belong to their metal clusters and organic linkers, which are sensitized and activated by visible light. In 2016, Chen and co-workers reported a microporous robust Zr-MOF as shown in **Figure 13**a, named NNU-28, was synthesized in a solvothermal reaction of $ZrCl_4$, H_2L (4, 4′-(diethynylanthracene-9,10diyl) dibenzoic acid) and benzoic acid in a DMF solution at 100 °C for 3 days.[65] The high surface area (≈1490 m^2 g^{-1}) NNU-28 showed a maximum CO_2 uptakes of 63.43 and 33.42 cm^3 g^{-1} at 273 and 298 K, respectively. The visible light absorption band of NNU-28 adsorbed further into the red wavelength than that the lone ligand from contributions of coordination between metal clusters and organic ligands, which agreed with their results of surface photovoltage spectroscopy. Thus NNU-28 can be applied as a highly efficient visible-light-responsive photocatalyst for the reduction of CO_2 to formate. The photocatalytic reaction condition was measured in a CH_3CN/TEOA

solution (v/v = 30/1) at room temperature under 1 bar CO_2. As illustrated in Figure 13b, the concentration of $HCOO^-$ indicated a time-dependent increase under visible-light, which generated 26.4 µmol $HCOO^-$ in 10 hours. The average formation rate was 183.3 µmol h^{-1} $mmol_{MOF}^{-1}$, which was higher than 46.3, 73.4, 71.9, and 143.5 µmol h^{-1} $mmol_{MOF}^{-1}$ for H_2N-UiO-66, mixed H_2-UiO-66, H_2N-UiO-66(Zr, Ti), and PCN-222, respectively. This high formation was attributed to the synergistic effect between the Zr_6 metal clusters and the anthracene-based ligands for visible light harvesting. To confirm the superiority of the MOF photocatalyst, control experiments were conducted for the anthracene-based ligand and separately without a catalyst. NNU-28 exhibited about three times more efficiency than the pure ligand. As shown in Figure 13c, a tentative mechanism of the dual photocatalytic routes for visible-light-driven CO_2 reduction in NNU-28 was proposed. Under the visible-light, the anthracene-based ligand assists the photoreduction of CO_2 both near the ligand (photoinduced charge generation) and by transferring energy to the Zr_6 cluster via ligand-to-metal charge transfer (LMCT). In addition, NH_2-MIL-101(Fe), NH_2-MIL-53(Fe), NH_2-MIL-88B(Fe),[70] and NH_2-MIL-125(Ti)[71] all exhibited high activity for photocatalytic CO_2 reduction via dual excitation pathways over amino-functionalized Fe- or Ti-based MOFs under visible-light irradiation (Figure 13d).

3.3. Metal-Decorated MOFs

At this time, heterogeneous MOF photocatalysts have been achieved by introducing photoactive catalytic sites (e.g., metal ions or metallolinkers) in MOF materials.[72–80] Lin
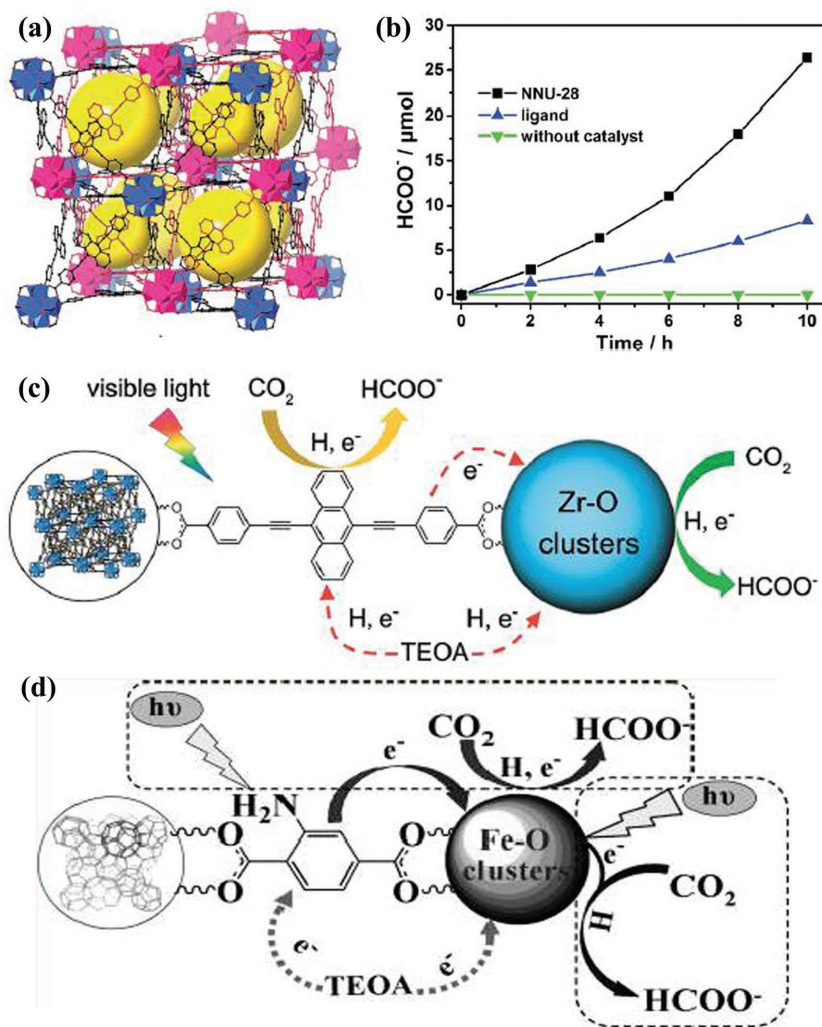
Figure 13. a) The structures of NNU-28 with two types of cages (yellow spheres represent void spaces). b) The amount of $HCOO^-$ produced as a function of irradiation time under different conditions. MeCN/TEOA (30/1), solution volume (60 mL), photocatalyst: NNU-28 (50 mg), and ligand (40.2 mg). c) A tentatively proposed mechanism of the dual photocatalytic routes for visible-light-driven CO_2 reduction in NNU-28.[65] Copyright 2016, the Royal Society of Chemistry. d) A tentative mechanism of the dual excitation pathways for visible-light-driven CO_2 reduction.[70] Copyright 2014, American Chemical Society.

and co-workers incorporated $Re(bpydc)(CO)_3Cl$ complexes into UiO-67 to achieve a photocatalytic MOF for CO_2 reduction to carbon monoxide (CO) using a mix-and-match synthetic strategy.[72] Motivated by the above example, intensive research efforts have been made to explore and synthesize such heterogeneous MOF photocatalysts for visible-light-driven CO_2 reduction. Kajiwara and co-workers introduced molecular catalyst $(Ru^{2+}(H_2bpydc)(terpy)(CO))(PF_6)_2$ or H_2RuCO complex (ligand modified from $(Ru^{2+}(bpy)(terpy)(CO))(PF_6)_2$ or Ru^{2+}-CO) via post-synthetic exchange into the UiO-67 framework forming Zr-bpdc/RuCO photocatalyst (**Figure 14**a).[73] The resulting material exhibited high catalytic activity for CO_2 photoreduction to CO, HCOOH and H_2. As the CO_2 concentration decreased, the catalytic activity of Ru^{2+}-CO and Zr-bpdc/RuCO also decreased (Figure 14b). When the CO_2 concentration was lower than 20% in a CO_2/Ar gas mixture, Zr-bpdc/RuCO showed higher catalytic performance than the discrete Ru^{2+}-CO catalyst. On the other hand, product selectivity is also very important in catalytic processes. As shown in Figure 14b, it was found that Zr-bpdc/RuCO can generate a larger amount of H_2 than Ru^{2+}-CO, which was mainly attributed to the Zr_6 metal clusters. More importantly, Zr-bpdc/RuCO showed a higher selectivity of CO/HCOOH than Ru^{2+}-CO under comparable conditions. This difference was due to an increase in CO_2 concentrations within the pores of the MOF nanoreactor. Many similar MOF
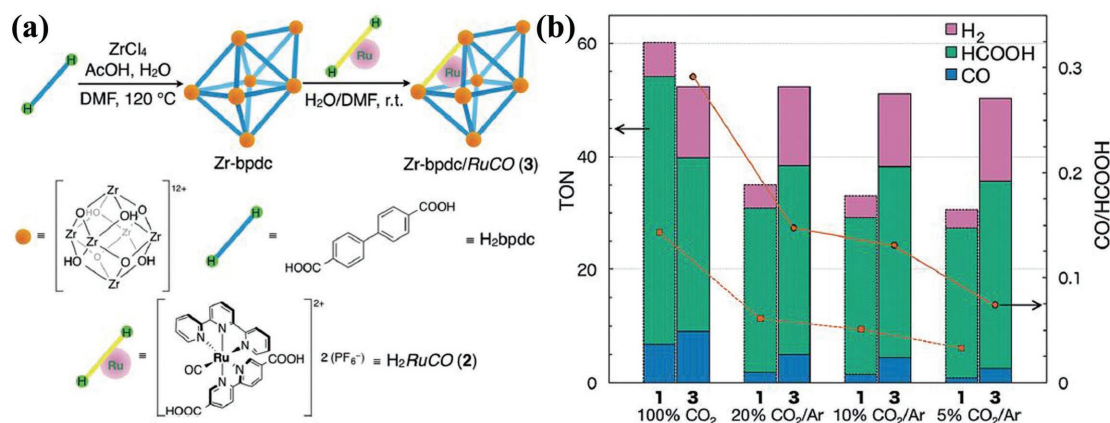

Figure 14. a) Synthesis of Zr-bpdc/RuCO by the post-synthetic exchange method of H_2RuCO with bpdc in UiO-67. b) Photochemical reduction of CO_2 with H_2RuCO and Zr-bpdc/RuCO: left y-axis, catalytic activity (bar graph); right y-axis, product selectivity (line graph). Reproduced with permission.[73] Copyright 2016, Wiley-VCH.
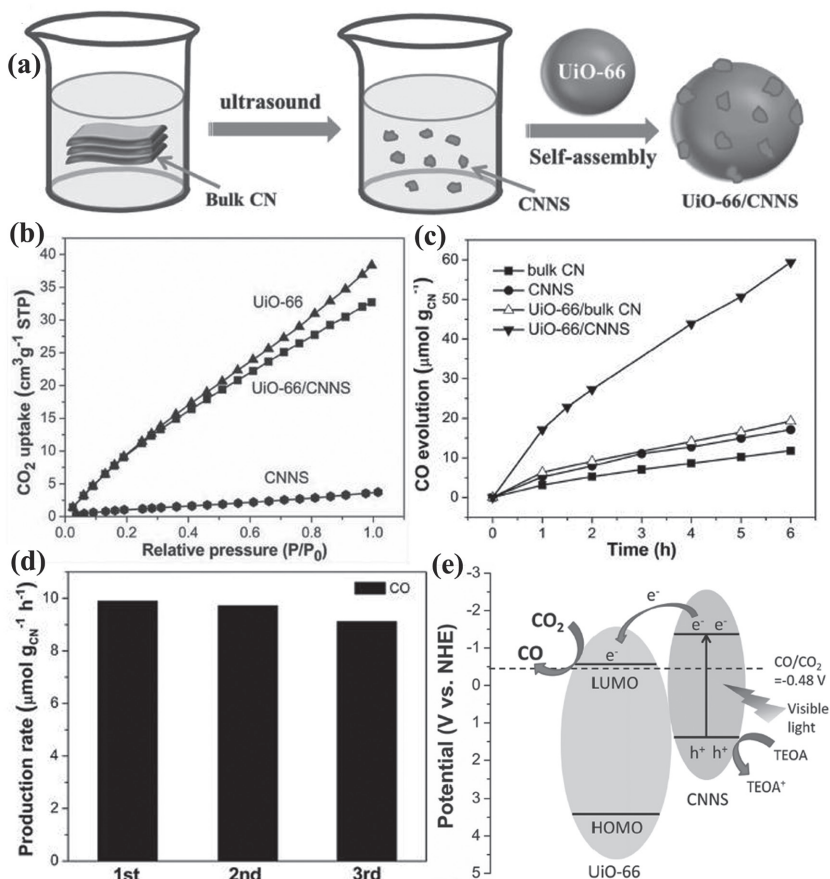
Figure 15. a) Schematic illustration of the preparation of the UiO-66/CNNS heterogeneous photocatalyst. b) CO_2 adsorption isotherms of UiO-66, CNNS, and UiO-66/CNNS at room temperature. c) Time course of CO evolution over bulk CN, CNNS, UiO-66/bulk CN, and UiO-66/CNNS photocatalysts. d) Production rate of CO over UiO-66/CNNS photocatalyst to measure reproducibility of cycling tests. For the hybrid structures, the CN content was 10 wt%. e) Proposed mechanism for photocatalytic CO_2 reduction to CO by UiO-66/CNNS heterogeneous photocatalyst under visible light irradiation. Reproduced with permission.[81] Copyright 2015, Wiley-VCH.

photocatalysts have been synthesized by Lin's group,[74] Cohen's group,[75,76] and Luo's group.[77,78]

3.4. Hybrid Photocatalysts Based on MOFs

MOFs combined with visible-light active photocatalysts are producing hybrid materials exhibiting high photocatalytic activity for CO_2 conversion.[81–83] Carbon nitride nanosheet (CNNS),[84] a metal-free and visible-light active photocatalyst, performs higher photocatalytic activity than graphitic carbon nitride (CN), but the efficiency for photocatalytic CO_2 is limited by the low capture of CO_2 gas. MOFs alleviate low CO_2 uptake where Shi and co-workers prepared a hybrid photocatalysts UiO-66/CNNS by an electrostatic self-assembly synthesis between positively charged UiO-66 and negatively charged CNNS.[81] As shown in **Figure 15**a, CNNSs dispersion are achieved during ultrasonic cavitation of bulk CN in water. Then, the resulting CNNS dispersion and UiO-66 are mixed and stirred in water to form

UiO-66/CNNS through an electrostatic self-assembly process. UiO-66/CNNS exhibited a higher CO_2 adsorption than CNNS due to the superior CO_2 uptake ability of UiO-66 crystals (Figure 15b). To evaluate the photocatalytic activity, all samples were investigated by the photocatalytic reduction of CO_2 to CO in a mild reaction containing triethanolamine (TEOA) as the electron donor. As shown in Figure 15c, UiO-66/CNNS demonstrated the highest CO yield of 59.4 μmol g_{CN}^{-1} under light irradiation for a duration of 6 hours outperforming UiO-66/bulk CN composite (19.3 μmol g_{CN}^{-1}), CNNS (17.1 μmol g_{CN}^{-1}), and bulk CN (12.1 μmol g_{CN}^{-1}). UiO-66/CNNS was demonstrated as durable from three photocatalytic cycles with the final cycle retaining much of the activity as the first (Figure 15d). To explain the outstanding catalytic activity of the UiO-66/CNNS composite, a mechanism was proposed for photocatalytic reduction of CO_2 to CO by UiO-66/CNNS photocatalyst under visible light irradiation in Figure 15e. Photogenerated electrons excited from the valence band of CNNS to its conduction band under visible irradiation are transferred to UiO-66 from the surface of CNNS at their interface. These electrons then reduce the adsorb CO_2 to CO. Finally, the electron donor TEOA can consume the remaining holes in CNNS. Similarly, Wang and colleagues also reported a hybrid MOF Co-ZIF-9 supporting CdS nanoparticles to aid in CO_2 reduction reactions.[82] Till now, many research efforts have been focused on developing MOFs for photocatalytic CO_2 reduction. However, just a few MOFs can be successfully applied as photocatalysts. Hence, more research is required to explore novel MOFs or their composites/hybrids photocatalysts experimentally or computationally.

4. CO_2 Chemically Fixated onto MOFs or Terminal Alkynes

Another strategy to chemically fix CO_2 as a C_1 building block, growing the molecule by one carbon atom, is to activate the C-H bond on terminal alkyne molecules allowing CO_2 to join as a carboxylate. For example, Liu and co-workers used MIL-101 as a host for growing Ag nanoparticles (NPs) in the crystalline material.[85] As shown in **Figure 16**a, an efficient heterogeneous catalyst, namely Ag@MIL-101, was successfully synthesized via a mild liquid impregnation-reduction approach to immobilize Ag NPs in MIL-101. The Ag NPs size distribution within the Ag@MIL-101 averaged 1.4(0.4) nm (Figure 16b and c), and showed a high CO_2 uptake.
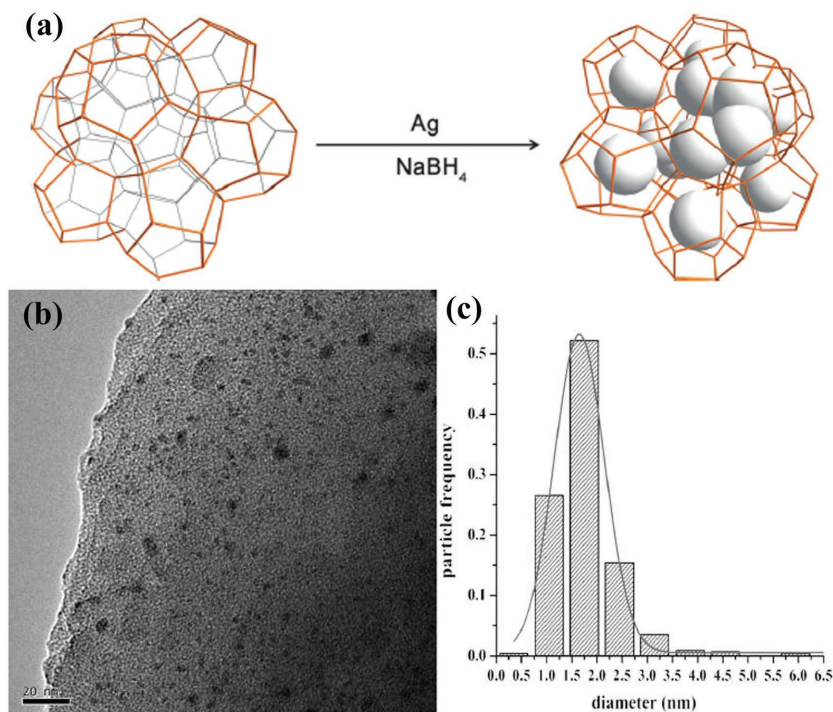
Figure 16. a) Schematic illustration of the synthesis of Ag@MIL-101 heterogeneous catalyst. b) TEM image of the Ag@MIL-101 catalyst. c) Size distribution of Ag NPs in the Ag@MIL-101 catalyst. Reproduced with permission.[85] Copyright 2015, Wiley-VCH.

Ag@MIL-101 catalyzed terminal alkynes into propiolic acid derivatives with high yields (>96%) in the present of Cs_2CO_3 under 1 atm CO_2 at 50°C in DMF after 15 hours. Ag@MIL-101 is easily separated from the reaction mixture by centrifugation and further recycled five additional times maintaining high catalytic activity. Their results demonstrated a useful approach to recycle silver nanoparticle in an efficient heterogeneous NPs@MOF catalysts and possible reduce the overall cost in CO_2 fixation reactions.

Gao and colleagues successfully inserted CO_2 onto the *aryl* C−H bonds on the dcppy ligand of UiO-67(dcppy) synthesizing a functional UiO-67(dcppy)-COOH MOF.[86] The carboxylate modified MOF then served as Brønsted acid sites to catalyze epoxide ring-opening reactions. As shown in

Figure 17a, the targeted framework UiO-67(dcppy)-COOH was achieved by mixing UiO-67(dcppy), chlorobis(cyclooctene)-rhodium(I) in *N,N′*-dimethylacetamide under 1 atm CO_2 at 90°C for 24 hours. PXRD and N_2 adsorption isotherm confirmed UiO-67(dcppy)-COOH retained its structure and permanent porosity. Ammonia temperature-programmed desorption (TPD) measurements proved the addition of free carboxylate groups on UiO-67(dcppy)-COOH from an addition desorption peak at 450 K. Ring-opening reaction yields of cyclohexene oxide by methanol approached 85%, which was better than controls from UiO-67(dcppy), dcppy, tcppy, and benzonic acid. Gao et al. proposed mechanism for chemical insertion of CO_2 at the *aryl* C−H bonds of UiO-67(dcppy) as shown in Figure 17b. This method expressed a new route to chemically fix CO_2 as a C_1 building block to modify MOFs for further applications. So far, only two research groups have reported on the CO_2 chemical fixation onto a MOF or a terminal alkyne. Many efforts should be focused on exploring other MOFs for similar CO_2 fixation reaction. In addition, theoretical research also should be systematic studied to guide future research in this scientific discipline.

5. Conclusions and Perspectives

MOF-based catalysts are quickly advancing carbon capture and storage/sequestration to alleviate CO_2 concerns and produce useful chemicals. While only a handful of MOFs have been applied for CO_2 chemical transformations over the past few years, this area is quickly becoming a distinguishing field in the MOF community. MOFs allow chemists and materials scientists to control and design the structures to give a
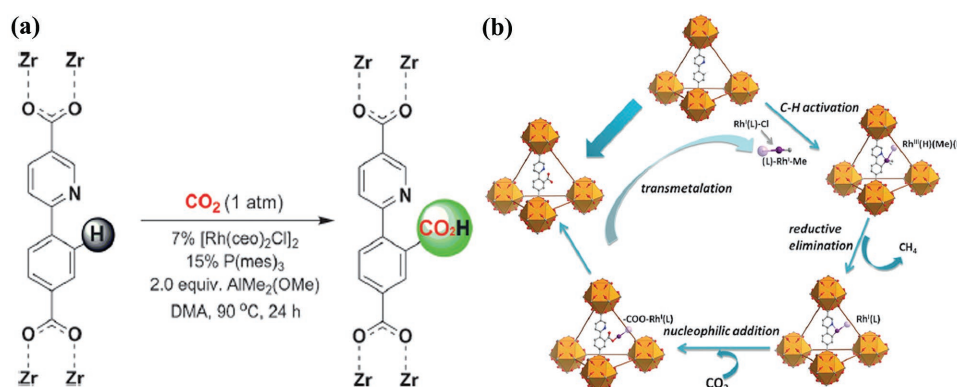

Figure 17. a) Schematic illustration of insertion of CO_2 into the aryl C-H bond within UiO-67(dcppy). b) A tentatively catalytic mechanism for chemical insertion of CO_2 into *aryl* C-H bonds of the UiO-67(dcppy) backbone. Reproduced with permission.[86] Copyright 2016, Wiley-VCH.

specific platform to perform a wide variety of applications in CO_2 conversion including the cycloaddition reaction of CO_2, electrocatalytic or photochemical reduction of CO_2, CO_2 fixation with terminal alkynes into propiolic acid derivatives and so many more. MOFs also provide a significant platform for in-depth investigations for the relationship between the catalytic performance and local reaction environment. This information is useful for optimizing the design of next-generation MOFs for a wider range of applications. As discussed in this review, MOFs feature many outstanding catalytic applications in CO_2 utilization. However, more research and development to use these materials as heterogeneous catalysts at the industrial scale needs to be developed.

This review provides a systematic overview on the development of MOF-based catalysts for CO_2 chemical transformations from the first example to the most recent publications. The strategies and approaches are discussed and studied in detail, which can be used to design and synthesize efficient MOF catalysts for using CO_2 as a carbon building block in organic materials. However, there is a still an immense challenge to prepare more MOF catalysts than the reported MOFs for CO_2 chemical transformations, operating the catalytic reactions under mild conditions, including low temperature, atmospheric pressure, and low CO_2 concentration. As a consequence, enhancing CO_2 uptake capacity is an essential point to address for promoting these CO_2 reactions because increasing the local CO_2 concentration around the activated sites should increase reaction yields.

In conclusion, MOFs applied as heterogeneous catalysts will continue to attract interest and research in converting CO_2 into valuable chemicals by academia and industry because of their unique and distinctive characteristics. It is an understatement to predict that MOFs will have a bright future for CO_2 chemical transformations in the industrial fields. However, extensive research should be explored and studied to overcome the drawbacks to construct practical MOFs as excellent catalysts in industry.

[1] S. Chu, *Science* **2009**, *325*, 1599.

[2] H. Yasuda, L. He, T. Sakakura, C. Hu, *J. Catal.* **2005**, *233*, 119.

[3] a) A. H. Lu, G. P. Hao, *Annu. Rep. Prog. Chem. Sect. A: Inorg. Chem.* **2013**, *109*, 484; b) Y. Zhang, B. Li, K. Williams, W. Y. Gao, S. Ma, *Chem. Commun.* **2013**, *49*, 10269.

[4] a) K. R. Thampi, J. Liwi, M. Grätzel, *Nature* **1987**, *327*, 506; b) M. R. Hudson, W. L. Queen, J. A. Mason, D. W. Fickel, R. F. Lobo, C. M. Brown, *J. Am. Chem. Soc.* **2012**, *134*, 1970.

[5] E. J. Doskocil, S. V. Bordawekar, B. G. Kaye, R. J. Davis, *J. Phys. Chem. B* **1999**, *103*, 6277.

[6] a) Y. Xie, T. T. Wang, X. H. Liu, K. Zou, W. Q. Deng, *Nat. Commun.* **2013**, *4*, 1960; b) W. Lu, J. P. Sculley, D. Yuan, R. Krishna, Z. Wei,

[7] a) H. Zhou, S. Kitagawa, *Chem. Soc. Rev.* **2014**, *43*, 5415; b) W. Lu, Z. Wei, Z. Y. Gu, T. F. Liu, J. Park, J. Park, J. Tian, M. Zhang, Q. Zhang, T. Gentle, M. Bosch, H. C. Zhou, *Chem. Soc. Rev.* **2014**, *43*, 5561.

[8] a) Q. Yang, D. Liu, C. Zhong, J. R. Li, *Chem. Rev.* **2013**, *113*, 8261; b) J. R. Li, R. J. Kuppler, H. C. Zhou, *Chem. Soc. Rev.* **2009**, *38*, 1477; c) H. He, Y. Song, C. Zhang, F. Sun, R. Yuan, Z. Bian, L. Gao, G. Zhu, *Chem. Commun.* **2015**, *51*, 9463.

[9] a) N. Ahmad, H. A. Younus, A. H. Chughtai, F. Verpoort, *Chem. Soc. Rev.* **2015**, *44*, 9; b) T. Baati, L. Njim, F. Neffati, A. Kerkeni, M. Bouttemi, R. Gref, M. F. Najjar, A. Zakhama, P. Couvreur, C. Serre, P. Horcajada, *Chem. Sci.* **2013**, *4*, 1597; c) H. Su, F. Sun, J. Jia, H. He, A. Wang, G. Zhu, *Chem. Commun.* **2015**, *51*, 5774.

[10] a) L. K. Kreno, K. Leong, O. K. Farha, M. Allendorf, R. P. V. Duyne, J. T. Hupp, *Chem. Rev.* **2012**, *112*, 1105; b) H. He, Y. Song, F. Sun, Z. Bian, L. Gao, G. Zhu, *J. Mater. Chem. A* **2015**, *3*, 16598; c) D. Banerjee, Z. Hu, J. Li, *Dalton Trans.* **2014**, *43*, 10668.

[11] a) J. Liu, L. Chen, H. Cui, J. Zhang, L. Zhang, X. Y. Su, *Chem. Soc. Rev.* **2014**, *43*, 6011; b) B. Li, K. Leng, Y. Zhang, J. J. Dynes, J. Wang, Y. Hu, D. Ma, Z. Shi, L. Zhu, D. Zhang, Y. Sun, M. Chrzanowski, S. Ma, *J. Am. Chem. Soc.* **2015**, *137*, 4243; c) A. M. Shultz, O. K. Farha, J. T. Hupp, S. T. Nguyen, *J. Am. Chem. Soc.* **2009**, *131*, 4204.

[12] a) P. Ramaswamy, N. E. Wong, G. K. H. Shimizu, *Chem. Soc. Rev.* **2014**, *43*, 5913; b) M. Sadakiyo, T. Yamada, H. Kitagawa, *J. Am. Chem. Soc.* **2014**, *136*, 13166; c) J. M. Taylor, R. K. Mah, I. L. Moudrakovski, C. I. Ratcliffe, R. Vaidhyanathan, G. K. H. Shimizu, *J. Am. Chem. Soc.* **2010**, *132*, 14055.

[13] O. M. Yaghi, M. O'Keeffe, N. W. Ockwing, H. K. Chae, M. Eddaoudi, J. Kim, *Nature* **2003**, *423*, 705.

[14] M. North, R. Pasquale, *Angew. Chem.* **2009**, *121*, 2990; *Angew. Chem. Int. Ed. Engl.* **2009**, *48*, 2946.

[15] A. J. Morris, G. J. Meyer, E. Fujita, *Acc. Chem. Res.* **2009**, *42*, 1983.

[16] D. J. Darensbourg, M. W. Holtcamp, *Coord. Chem. Rev.* **1996**, *153*, 155.

[17] M. H. Beyzavi, C. J. Stephenson, Y. Liu, O. Karagiaridi, J. T. Hupp, O. K. Farha, *Front. Energy Res.* **2015**, *2*, 63.

[18] J. Song, Z. Zhang, S. Hu, T. Wu, T. Jiang, B. Han, *Green. Chem.* **2009**, *11*, 1301.

[19] C. M. Miralda, E. E. Macias, M. Zhu, P. Ratnasamy, M. A. Carreon, *ACS Catal.* **2012**, *2*, 180.

[20] L. Yang, L. Yu, G. Diao, M. Sun, G. Cheng, S. Chen, *J. Mol. Catal. A: Chem.* **2014**, *392*, 278.

[21] B. Mousavi, S. Chaemchuen, B. Moosavi, Z. Luo, N. Gholampour, F. Verpoort, *New J. Chem.* **2016**, *40*, 5170.

[22] R. R. Kuruppathparambil, T. Jose, R. Babu, G. Y. Hwang, A. C. Kathalikkattil, D. W. Kim, D. W. Park, *Appl. Catal. A: Gen.* **2016**, *182*, 562.

[23] J. Tharun, G. Mathai, A. C. Kathlikkattil, R. Roshan, Y.-S. Won, S. J. Cho, J.-S. Chang, D. W. Park, *ChemPlusChem* **2015**, *80*, 715.

[24] Z. Zhou, C. He, J. Xiu, L. Yang, C. Duan, *J. Am. Chem. Soc.* **2015**, *137*, 15066.

[25] V. Guillerm, L. J. Weseliński, Y. Belmabkhout, A. J. Cairns, V. D'Elia, L. Wojtas, K. Adil, M. Eddaoudi, *Nat. Chem.* **2014**, *6*, 673.

[26] R. Zou, P. Z. Yi, Y. F. Zeng, J. Liu, R. Zhao, H. Duan, Z. Luo, J. G. Wang, R. Zou, Y. Zhao, *Small* **2016**, *12*, 2334.

[27] M. H. Beyzavi, R. C. Klet, S. Tussupbayev, J. Borycz, N. A. Vermeulen, C. J. Cramer, J. F. Stoddart, J. T. Hupp, O. K. Farha, *J. Am. Chem. Soc.* **2014**, *136*, 15861.

[28] Z. R. Jiang, H. Wang, Y. Hu, J. Lu, H. L. Jiang, *ChemSusChem* **2015**, *8*, 878.

[29] A. C. Kathalikkattil, R. Roshan, J. Tharun, R. Babu, G.-S. Jeong, D.-W. Kim, S. J. Cho, D. W. Park, *Chem. Commun.* **2016**, *52*, 280.

[30] A. C. Kathalikkattil, R. Babu, R. K. Roshan, H. Lee, H. Kim, J. Tharun, E. Suresh, D.-W. Park, *J. Mater. Chem. A* **2015**, *3*, 22636.

[31] L. Liu, S. M. Wang, Z. B. Han, M. Ding, D. Q. Yuan, H. L. Jiang, *Inorg. Chem.* **2016**, *55*, 3558.

[32] D. A. Yang, H. Y. Cho, J. Kim, S. T. Yang, W. S. Ahn, *Energy Environ. Sci.* **2012**, *5*, 6465.

[33] B. Zou, L. Hao, L. Y. Fan, Z. M. Gao, S. L. Chen, H. Li, C. W. Hu, *J. Catal.* **2015**, *329*, 119.

[34] F. Liu, Y. Xu, L. Zhao, L. Zhang, W. Guo, R. Wang, D. Sun, *J. Mater. Chem. A* **2015**, *3*, 21545.

[35] S. Kumar, G. Verma, W. Y. Gao, Z. Niu, L. Wojtas, S. Ma, *Eur. J. Inorg. Chem.*, DOI: 10.1002/ejic.201600218.

[36] A. C. Kathalikkattil, D. W. Kim, J. Tharun, H. G. Soek, R. Roshan, D. W. Park, *Green Chem.* **2014**, *16*, 1607.

[37] X. Huang, Y. Chen, Z. Lin, X. Ren, Y. Song, Z. Xu, X. Dong, X. Li, C. Hu, B. Wang, *Chem. Commun.* **2014**, *50*, 2624.

[38] W. Y. Gao, L. Wojtas, S. Ma, *Chem. Commun.* **2014**, *50*, 5316.

[39] D. Feng, W. C. Chung, Z. Wei, Z. Y. Gu, H. L. Jiang, J. P. Chen, D. J. Darensbourg, H. C. Zhou, *J. Am. Chem. Soc.* **2013**, *135*, 17105.

[40] W. Y. Gao, C. Y. Tsai, L. Wojtas, T. Thiounn, C. C. Lin, S. Ma, *Inorg. Chem.* **2016**, *55*, 7291.

[41] Y. Ren, Y. Shi, J. Chen, S. Yang, C. Qi, H. Jiang, *RSC Advances* **2013**, *3*, 2167.

[42] W. Y. Gao, Y. Chen, Y. Niu, K. Williams, L. Cash, P. J. Perez, L. Wojtas, J. Cai, Y. S. Chen, S. Ma, *Angew. Chem.* **2014**, *126*, 2653; *Angew. Chem. Int. Ed. Engl.* **2014**, *53*, 2615.

[43] D. Ma, B. Li, K. Liu, X. Zhang, W. Zou, Y. Yang, G. Li, Z. Shi, S. Feng, *J. Mater. Chem. A* **2015**, *3*, 23136.

[44] X. Zhou, Y. Zhang, X. Yang, L. Zhao, G. Wang, *J. Mol. Catal. A: Chem.* **2012**, *361–362*, 12.

[45] T. Jose, Y. Hwang, D. W. Kim, M. I. Kim, D. W. Park, *Catal. Today* **2015**, *245*, 61.

[46] J. Tharun, K. M. Bhin, R. Roshan, D. W. Kim, A. C. Kathalikkattil, R. Babu, H. Y. Ahn, Y. S. Won, D. W. Park, *Green Chem.* **2016**, *18*, 2479.

[47] T. Lescouet, C. Chizallet, D. Farrusseng, *ChemCatChem* **2012**, *4*, 1725.

[48] J. Kim, S. N. Kim, H. G. Jang, G. Seo, W. S. Ahn, *Appl. Catal. A: Gen.* **2013**, *453*, 175.

[49] R. Babu, A. C. Kathalikkattil, R. Roshan, J. Tharun, D. W. Kim, D. W. Park, *Green Chem.* **2016**, *18*, 232.

[50] P. Z. Li, X. J. Wang, J. Liu, J. S. Lim, R. Zou, Y. Zhao, *J. Am. Chem. Soc.* **2016**, *138*, 2142.

[51] W. Kleist, F. Jutz, M. Maciejewski, A. Baiker, *Eur. J. Inorg. Chem.* **2009**, 3552.

[52] L. Liu, J. Zhang, H. Fang, L. Chen, C. Y. Su, *Chem. Asian J.*, DOI: 10.1002/asia.201600698.

[53] L. Song, C. Chen, X. Chen, N. Zhang, *New J. Chem.* **2016**, *40*, 2904.

[54] Y. H. Han, Z. Y. Zhou, C. B. Tian, S. W. Du, *Green Chem.* **2016**, *18*, 4086.

[55] a) C. D. Windle, R. N. Perutz, *Coord. Chem. Rev.* **2012**, *256*, 2562; b) N. S. Lewis, D. G. Nocera, *Proc. Natl. Acad. Sci. USA* **2006**, *103*, 15729.

[56] T. Sakakura, J. C. Choi, H. Yasuda, *Chem. Rev.* **2007**, *107*, 2365.

[57] R. S. Kumar, S. S. Kumar, M. A. Kulandainathan, *Electrochem. Commun.* **2012**, *25*, 70.

[58] N. Kornienko, Y. Zhao, C. S. Kley, C. Zhu, D. Kim, S. Lin, C. J. Chang, O. M. Yaghi, P. Yang, *J. Am. Chem. Soc.* **2015**, *137*, 14129.

[59] J. Albo, D. Vallejo, G. Beobide, O. Castillo, P. Castano, A. Irabien, *ChemSusChem* **2016**, *9*, 1.

[60] R. Hinogami, S. Yotsuhashi, M. Deguchi, Y. Zenitani, H. Hashiba, Y. Yamada, *ECS Electrochem. Lett.* **2012**, *1*, H17.

[61] I. Hod, M. D. Sampson, P. Deria, C. P. Kubiak, O. K. Farha, J. T. Hupp, *ACS Catal.* **2015**, *5*, 6302.

[62] a) A. Doménech, H. García, M. T. Doménech-Carbó, F. Llabrés-i-Xamena, *J. Phys. Chem. C* **2007**, *111*, 13701; b) T. Maihom, S. Wannakao, B. Boekfa, J. Limtrakul, *J. Phys. Chem. C* **2013**, *117*, 17650; c) I. Hod, P. Deria, W. Bury, J. E. Mondloch, C. W. Kung, M. So, M. D. Sampson, A. W. Peters, C. P. Kubiak, O. K. Farha, J. R. Hupp, *Nat. Commun.* **2015**, *6*, 8304; d) S. Lin, C. S. Diercks, Y. B. Zhang, N. Kornienko, E. M. Nichols, Y. Zhao, A. R. Paris, D. Kim, P. Yang, O. M. Yaghi, C. J. Chang, *Science* **2015**, *349*, 1208.

[63] a) V. P. Indrakanti, J. D. Kubicki, H. H. Schobert, *Energy Environ. Sci.* **2009**, *2*, 745; b) T. Inoue, A. Fujishima, S. Konishi, K. Honda, *Nature* **1979**, *277*, 637; c) K. R. Thampi, J. Kiwi, M. Gratzel, *Nature* **1987**, *327*, 506.

[64] a) J. Ettedgui, Y. Diskin-Posner, L. Weiner, R. Neumann, *J. Am. Chem. Soc.* **2011**, *133*, 188; b) J. M. Lehn, R. Ziessel, *Proc. Natl. Acad. Sci. USA* **1982**, *79*, 701; c) Y. Tamaki, T. Morimoto, K. Koite, O. Ishitani, *Proc. Natl. Acad. Sci. USA* **2012**, *109*, 15673.

[65] D. Chen, H. Xing, C. Wang, Z. Su, *J. Mater. Chem. A* **2016**, *4*, 2657.

[66] Y. Lee, S. Kim, J. K. Kang, S. M. Cohen, *Chem. Commun.* **2015**, *51*, 5735.

[67] D. Sun, Y. Fu, W. Liu, L. Ye, D. Wang, L. Yang, X. Fu, Z. Li, *Chem. Eur. J.* **2013**, *19*, 14279.

[68] D. Sun, W. Liu, M. Qiu, Y. Zhang, Z. Li, *Chem. Commun.* **2015**, *51*, 2056.

[69] H. Q. Xu, J. Hu, D. Wang, Z. Li, Q. Zhang, Y. Luo, S. H. Yu, H. L. Jiang, *J. Am. Chem. Soc.* **2015**, *137*, 13440.

[70] D. Wang, R. Huang, W. Liu, D. Sun, Z. Li, *ACS Catal.* **2014**, *4*, 4254.

[71] Y. Fu, D. Sun, Y. Chen, R. Huang, Z. Ding, X. Fu, Z. Li, *Angew. Chem.* **2012**, *124*, 3420; *Angew. Chem. Int. Ed. Engl.* **2012**, *51*, 3364.

[72] C. Wang, Z. Xie, K. E. deKrafft, W. Lin, *J. Am. Chem. Soc.* **2011**, *133*, 13445.

[73] T. Kajiwara, M. Fujii, M. Tsujimoto, K. Kobayashi, M. Higuchi, K. Tanaka, S. Kitagawa, *Angew. Chem.* **2016**, *128*, 2747; *Angew. Chem. Int. Ed. Engl.* **2016**, *55*, 2697.

[74] R. Huang, Y. Peng, C. Wang, Z. Shi, W. Lin, *Eur. J. Inorg. Chem.*, DOI: 10.1002/ejic.201600064.

[75] Y. Lee, S. Kim, H. Fei, J. K. Kang, S. M. Cohen, *Chem. Commun.* **2015**, *51*, 16549.

[76] H. Fei, M. D. Sampson, Y. Lee, C. P. Kubiak, S. M. Cohen, *Inorg. Chem.* **2015**, *54*, 6821.

[77] S. Zhang, L. Li, S. Zhao, Z. Sun, J. Luo, *Inorg. Chem.* **2015**, *54*, 8375.

[78] L. Li, S. Zhang, L. Xu, J. Wang, L. X. Shi, Z. N. Chen, M. Hong, J. Luo, *Chem. Sci.* **2014**, *5*, 3808.

[79] D. Sun, Y. Gao, J. Fu, X. Zeng, Z. Chen, Z. Li, *Chem. Commun.* **2015**, *51*, 2645.

[80] M. B. Chambers, X. Wang, N. Elgrishi, C. H. Hendon, A. Walsh, J. Bonnefoy, J. Canivet, E. A. Quadrelli, D. Farrusseng, C. Mellot-Draznieks, M. Fontecave, *ChemSusChem* **2015**, *8*, 603.

[81] L. Shi, T. Wang, H. Zhang, K. Chang, J. Ye, *Adv. Funct. Mater.* **2015**, *25*, 5360.

[82] S. Wang, X. Wang, *Appl. Catal. B: Environ.* **2015**, *162*, 494.

[83] P. Wu, X. Guo, L. Cheng, C. He, J. Wang, C. Duan, *Inorg. Chem.* **2016**, *55*, 8153.

[84] a) S. Yang, Y. Gong, J. Zhang, L. Zhan, L. Ma, Z. Fang, R. Vajtai, X. Wang, P. M. Ajayan, *Adv. Mater.* **2013**, *25*, 2452; b) P. Niu, L. Zhang, G. Liu, H. M. Cheng, *Adv. Funct. Mater.* **2012**, *22*, 4763; c) X. Lu, K. Xu, P. Chen, K. Jia, S. Liu, C. Wu, *J. Mater. Chem. A* **2014**, *2*, 18924.

[85] X. H. Liu, J. G. Ma, Z. Niu, G. M. Yang, P. Cheng, *Angew. Chem.* **2015**, *127*, 1002; *Angew. Chem. Int. Ed. Engl.* **2015**, *54*, 988.

[86] W. Y. Gao, H. Wu, K. Leng, Y. Sun, S. Ma, *Angew. Chem.* **2016**, *128*, 5562; *Angew. Chem. Int. Ed. Engl.* **2016**, *55*, 5472.